ORGANOMETALLICS

Article

pubs.acs.org/Organometallics

Rh–POP Pincer Xantphos Complexes for C–S and C–H Activation. Implications for Carbothiolation Catalysis

Peng Ren,† Sebastian D. Pike, Indrek Pernik, Andrew S. Weller,* and Michael C. Willis

Department of Chemistry, Chemistry Research Laboratories, Mansfield Road, University of Oxford, Oxford, OX1 3TA, U.K.

Supporting Information

ABSTRACT: The neutral Rh(I)–Xantphos complex [Rh(κ^3-$_{P,O,P}$-Xantphos)Cl]$_n$, **4**, and cationic Rh(III) [Rh(κ^3-$_{P,O,P}$-Xantphos)(H)$_2$][BAr$^F_4$], **2a**, and [Rh(κ^3-$_{P,O,P}$-Xantphos-3,5-C$_6$H$_3$(CF$_3$)$_2$)(H)$_2$][BAr$^F_4$], **2b**, are described [Ar^F = 3,5-(CF$_3$)$_2$C$_6$H$_3$; Xantphos = 4,5-bis(diphenylphosphino)-9,9-dimethylxanthene; Xantphos-3,5-C$_6$H$_3$(CF$_3$)$_2$ = 9,9-dimethylxanthene-4,5-bis(bis(3,5-bis(trifluoromethyl)phenyl)phosphine]. A solid-state structure of **2b** isolated from C$_6$H$_5$Cl solution shows a κ^1-chlorobenzene adduct, [Rh(κ^3-$_{P,O,P}$-Xantphos-3,5-C$_6$H$_3$(CF$_3$)$_2$)(H)$_2$(κ^1-ClC$_6$H$_5$)][BAr$^F_4$], **3**. Addition of H$_2$ to **4** affords, crystallographically characterized, [Rh(κ^3-$_{P,O,P}$-Xantphos)(H)$_2$Cl], **5**. Addition of diphenyl acetylene to **2a** results in the formation of the C–H activated metallacyclopentadiene [Rh(κ^3-$_{P,O,P}$-Xantphos)(ClCH$_2$Cl)(σ,σ-(C$_6$H$_4$)C(H)=CPh)][BAr$^F_4$], **7**, a rare example of a crystallographically characterized Rh–dichloromethane complex, alongside the Rh(I) complex *mer*-[Rh(κ^3-$_{P,O,P}$-Xantphos)(η^2-PhCCPh)][BAr$^F_4$], **6**. Halide abstraction from [Rh(κ^3-$_{P,O,P}$-Xantphos)Cl]$_n$ in the presence of diphenylacetylene affords **6** as the only product, which in the solid state shows that the alkyne binds perpendicular to the κ^3-POP Xantphos ligand plane. This complex acts as a latent source of the [Rh(κ^3-$_{P,O,P}$-Xantphos)]$^+$ fragment and facilitates *ortho*-directed C–S activation in a number of 2-arylsulfides to give *mer*-[Rh(κ^3-$_{P,O,P}$-Xantphos)(σ,κ^1-Ar)(SMe)][BAr$^F_4$] (Ar = C$_6$H$_4$COMe, **8**; C$_6$H$_4$(CO)OMe, **9**; C$_6$H$_4$NO$_2$, **10**; C$_6$H$_4$CNCH$_2$CH$_2$O, **11**; C$_6$H$_4$C$_5$H$_4$N, **12**). Similar C–S bond cleavage is observed with allyl sulfide, to give *fac*-[Rh(κ^3-$_{P,O,P}$-Xantphos)(η^3-C$_3$H$_5$)(SPh)][BAr$^F_4$], **13**. These products of C–S activation have been crystallographically characterized. For **8** in situ monitoring of the reaction by NMR spectroscopy reveals the initial formation of *fac*-κ^3-**8**, which then proceeds to isomerize to the *mer*-isomer. With the *para*-ketone aryl sulfide, 4-SMeC$_6$H$_4$COMe, C–H activation *ortho* to the ketone occurs to give *mer*-[Rh(κ^3-$_{P,O,P}$-Xantphos)(σ,κ^1-4-(COMe)C$_6$H$_3$SMe)(H)][BAr$^F_4$], **14**. The temporal evolution of carbothiolation catalysis using *mer*-κ^3-**8**, and phenyl acetylene and 2-(methylthio)acetophenone substrates shows initial fast catalysis and then a considerably slower evolution of the product. We suggest that the initially formed *fac*-isomer of the C–S activation product is considerably more active than the *mer*-isomer (i.e., *mer*-**8**), the latter of which is formed rapidly by isomerization, and this accounts for the observed difference in rates. A likely mechanism is proposed based upon these data.

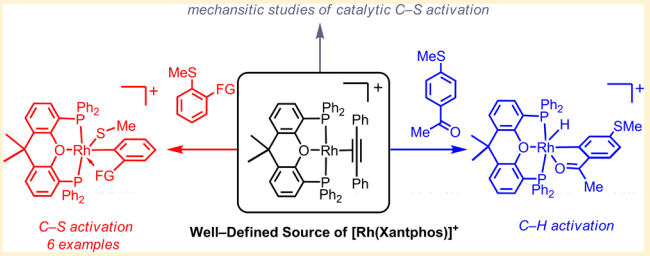

1. INTRODUCTION

The transition-metal chemistry associated with diphosphine, and related, pincer ligands is significant to many areas of organometallic chemistry, catalysis, and materials science. This is due to the attractive properties that such ligands give the resulting metal complexes, for example: stability, electronic and steric variability, and, in some cases, metal–ligand cooperativity.[1−5] Central to many of these studies have been systems based around "PCP" and "PNP"-type ligand scaffolds (Figure 1). These provide relatively rigid ligand environments, that often result in *mer*-κ^3-coordination geometries at the metal center. A less explored class of pincer ligand comes from POP-frameworks based upon the Xantphos-motif (Xantphos = 4,5-bis(diphenylphosphino)-9,9-dimethylxanthene, Figure 1),[6,7] that although originally developed to be *cis*-chelating bidentate phosphine ligands can also act as *mer*-κ^3 [8] or, less commonly, *fac*-κ^3 POP-pincer ligands.[9] Recently there has been significant interest in the chemistry associated with Xantphos acting as a POP-pincer ligand to the group 9 metals (Figure 2), for example in carbonylation (**A**),[9] activation of H$_2$/alkenes (**B**–**D**),[10−12] silylation (**E**),[13] hydroamination (**F**),[14] hydroacylation (**G**),[15] and amine–borane dehydrocoupling and hydroboration processes (**H**).[16−18]

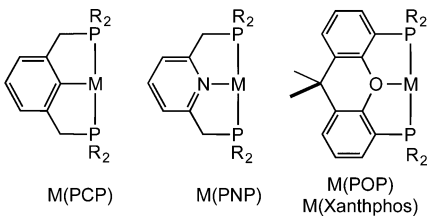

Figure 1. M(PCP), M(PNP), and M(POP) metal–ligand motifs.

We have recently reported the use of the [Rh(Xantphos)]$^+$ catalyst fragment in carbothiolation reactions between alkynes

Received: September 29, 2014
Published: February 9, 2015

DOI: 10.1021/om500984y
Organometallics 2015, 34, 711–723

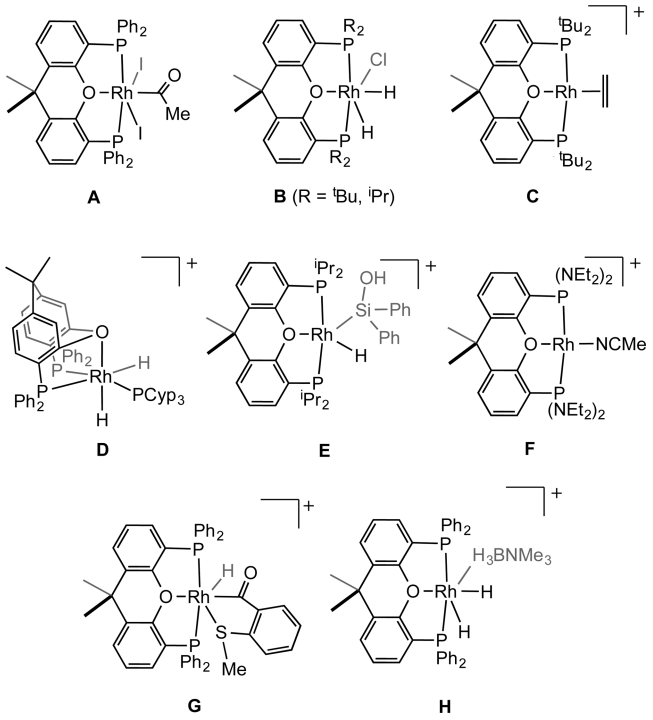

Figure 2. Representative examples of κ^3-Xantphos complexes.

and ketone-bearing aryl sulfides to produce alkenyl sulfide products (Scheme 1).[19] These catalyst systems operate best at elevated temperatures, e.g. coupling phenyl acetylene and 2-(methylthio)acetophenone at 373 K in chlorobenzene or dichloroethane solvent. In addition to this atom-efficient C–C and C–S bond formation process, the resulting alkenyl sulfide can be used for further functionalization, i.e. functional group recycling. This Xantphos system delivers improved yields and conversion times compared to our previously reported DPEphos system[20] [cf. Xantphos 99%, 2 h; DPEphos 90%, 24 h, Scheme 1, DPEphos = oxidi-2,1-phenylene-bis-(diphenylphosphine)]. For the DPEphos catalyst, *in situ* NMR spectroscopic studies identified the C–S activated intermediates *fac*-κ^3-**I** and *mer*-κ^3-**J** to be in equilibrium with one another at 298 K, while at 333 K *mer*-κ^3-**J** was the observed resting-state during catalysis.[20]

Transition-metal-catalyzed C–S activation processes are becoming increasingly important in synthesis,[21] especially their use in cross coupling reactions.[22−26] In this contribution we describe a study of the C–S activation processes occurring in the [Rh(Xantphos)][BAr^F_4] system. We also report a new, readily accessible, Rh(I)–Xantphos precursor complex which has a labile alkyne ligand; report C–H activation processes mediated by this fragment; and also make comment upon the likely active species in carbothiolation catalysis.

Scheme 1. Carbothiolation Using Rh–DPEphos and Xantphos Catalysts[a]

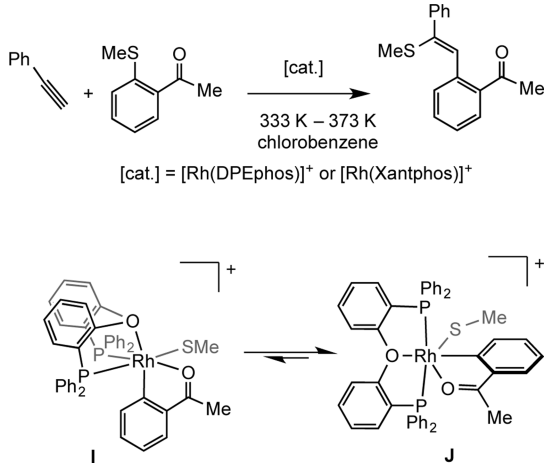

[a] $[BAr^F_4]^-$ anions are not shown.

2. RESULTS AND DISCUSSION

2.1. Synthesis of Rh(I) Precursor Complexes. A suitable entry point into the C–S activation chemistry would be a Rh(I) precursor that can promote oxidative addition of the ketosulfide substrate. Previously in the DPEphos system we used the *ortho*-xylene-ligated [Rh(κ^2-$_{P,P}$-DPEphos)(*o*-xylene)][BAr^F_4] as a suitable precursor. This was generated by addition of H_2 to the corresponding NBD complex in *o*-xylene (NBD = norbornadiene).[20] Noting that our recent report of the alkyne carbothiolation catalyzed by [Rh(Xantphos)]$^+$ used chlorobenzene as a solvent, we targeted an appropriate precursor that involved this as a ligand. Addition of H_2 to previously reported *cis*-[Rh(κ^2-$_{P,P}$-Xantphos)(NBD)][BAr^F_4], **1a**,[15] in C_6H_5Cl solvent resulted in the quantitative formation of a Rh(III) dihydride complex [Rh(κ^3-$_{P,O,P}$-Xantphos)$(H)_2$][BAr^F_4], **2a**, as characterized by *in situ* ^1H and $^{31}P\{^1H\}$ NMR spectroscopy (Scheme 2), which is analogous to recently reported variants Xantphos-^{t}Bu[11] or Xantphos-^{i}Pr[11]. Complex **2a** could not be isolated as a solid. However, treatment of the 3,5-$C_6H_3(CF_3)_2$ P-substituted Xantphos analog of **1a** (complex **1b**) with H_2 in C_6H_5Cl solution led to the isolation of [Rh(κ^3-$_{P,O,P}$-Xantphos-3,5-$C_6H_3(CF_3)_2$)$(H)_2$(κ^1-ClC_6H_5)][BAr^F_4], **3**, as a white crystalline solid in 79% yield. The solid-state structure of the cation as determined by single crystal X-ray diffraction is shown in Figure 3.

Scheme 2. Synthesis of Rh(III) Dihydride Xantphos Complexes[a]

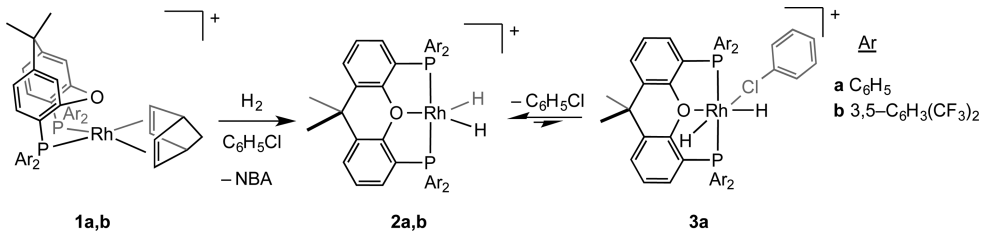

[a] $[BAr^F_4]^-$ anions are not shown.

DOI: 10.1021/om500984y
Organometallics 2015, 34, 711–723

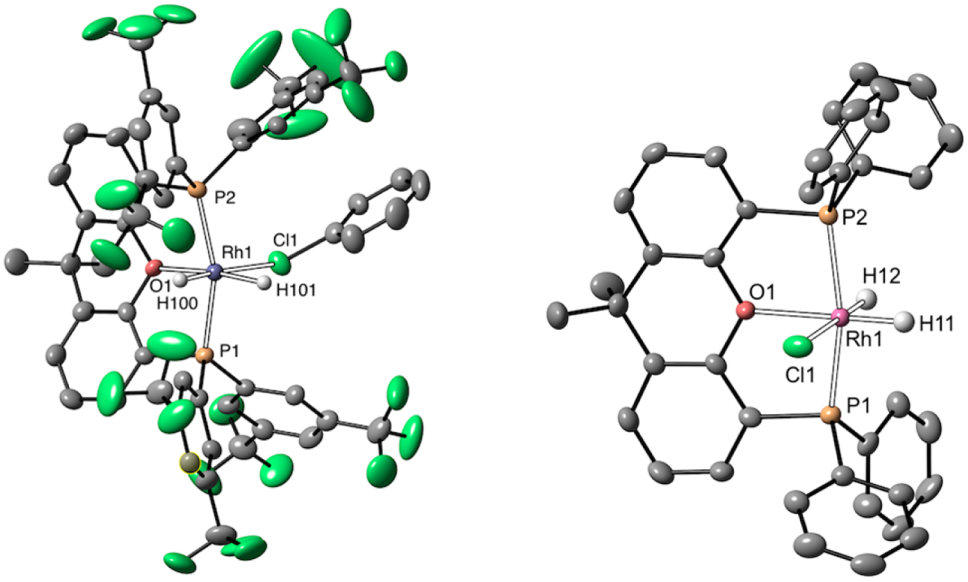

Figure 3. Solid-state structure of the cations in complexes **3** (left) and **5** (right). Displacement ellipsoids are shown at the 50% probability level. Most hydrogen atoms are not shown. Selected bond lengths (Å) and angles (deg): (**3**): Rh1−P1, 2.2673(12); Rh1−P2, 2.2707(13); Rh1−Cl1, 2.5207(12); Rh1−O1, 2.249(3); P1−Rh1−P2, 161.03(4); O1−Rh1−C1, 90.16(8). (**5**): Rh1−P1, 2.2591(10); Rh1−P2, 2.2779(11); Rh1−Cl1, 2.4625(11); Rh1−O1, 2.248(3); P1−Rh1−P2, 163.85(4); O1−Rh1−C1, 86.87(8).

The solid-state structure of **3** shows a *cis*-dihydride species (the hydrides were located in the difference map), with a κ^1-chlorobenzene [Rh−Cl 2.5207(12) Å] and a *mer*-κ^3-Xantphos ligand. Complex **3** is closely related to similar compounds in which acetone, MeCN,[15] or $H_3B{\cdot}NMe_3$[16] replace the chlorobenzene ligand, and the gross structural metrics are similar to these adducts. In the ^{1}H NMR spectrum of complex **3** in C_6D_5Cl solution, a single environment, indicated by a broad signal at δ −17.7, is observed for the hydride ligand, and a single Xantphos-methyl signal (6 H) is observed. A single environment showing coupling to ^{103}Rh [δ 45.3, J(RhP) = 118 Hz] is also observed in the ^{31}P{^{1}H} NMR spectrum. These data suggest a time-averaged C_{2v} symmetry for the metal fragment, likely approximated to a 5-coordinate "Y-shaped" [Rh(κ^3-$_{P,O,P}$-Xantphos-3,5-$C_6H_3(CF_3)_2$)$(H)_2$][$BAr^F{}_4$], i.e. **2b**. When complex **3** is dissolved in CD_2Cl_2, a signal assigned to free C_6H_5Cl is observed, in addition to very similar NMR spectroscopic data to **2a** in CH_2Cl_2 solution. Complexes **2a**/**b** in solution, or **3** in the solid state, do not lose H_2 on application of a vacuum (~10^{-3} Torr). Cooling of **3** (183 K, CD_2Cl_2) did not result in a ^{1}H NMR spectrum that reflects the solid-state structure (i.e., inequivalent hydrides were not observed). This is in contrast to [Rh(κ^3-$_{P,O,P}$-Xantphos)$(H)_2$(acetone)][$BAr^F{}_4$],[15] in which the hydrides are equivalent at 298 K but inequivalent at low temperature, which is suggested to be due to reversible decoordination of acetone. Given these data, we suggest that complex **3** exists in C_6H_5Cl or CD_2Cl_2 solution predominantly as [Rh(κ^3-$_{P,O,P}$-Xantphos-3,5-$C_6H_3(CF_3)_2$)$(H)_2$][$BAr^F{}_4$], **2b**, but can be recrystallized from C_6H_5Cl solvent to give the solvent adduct **3**. We discount a time-averaged six-coordinate complex with *trans*-hydrides as this would likely have a chemical shift for the hydride ligands at higher field than is observed [e.g., [Rh(κ^3-$_{P,O,P}$-Xantphos-^{t}Bu)$(H)_2(OH_2)$][SbF_6] δ −9].[11] Complex **3** adds to the very small number of crystallographically characterized κ^1-chlorobenzene complexes.[27] We cannot comment on whether a similar complex would be formed with **2a**, as we have been unable to produce crystalline material suitable for analysis.

As noted recently by Goldman, the formation of a Rh(III) dihydride complex over a Rh(I) species on addition of H_2 could well be due to the relatively weak *trans*-influence of the POP−ether ligating group in Xantphos that favors the product of oxidative addition of H_2.[11] In addition to this, wide-bite angle ligands such as Xantphos will tend to favor Rh(III) (dihydrides) over Rh(I) species.[28] Thus, avoiding the use of H_2 in the production of the precursor for C−S activation would thus be advantageous in generating a Rh(I) precursor. To accomplish this, addition of Xantphos to $[Rh(COE)_2Cl]_2$ (COE = cyclooctene) in C_6H_6 solution resulted in the formation of an insoluble (benzene) material that we tentatively characterize as the Rh(I) complex [Rh(Xantphos)-Cl]$_n$, **4**, presumably formed as a coordination polymer with bridging halide ligands (Scheme 3), based upon its insolubility. This material analyzed correctly for composition by elemental analysis. Dissolution in CH_2Cl_2 resulted in a mixture of, uncharacterized, products. Interestingly, the analogous com-

Scheme 3. Scheme Relating the Synthesis of Complexes 4, 5, 6, and 7[a]

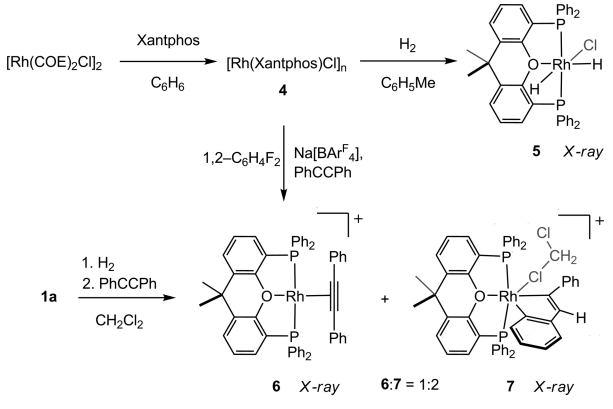

[a] $[BAr^F{}_4]^-$ anions are not shown.

DOI: 10.1021/om500984y
Organometallics 2015, 34, 711−723

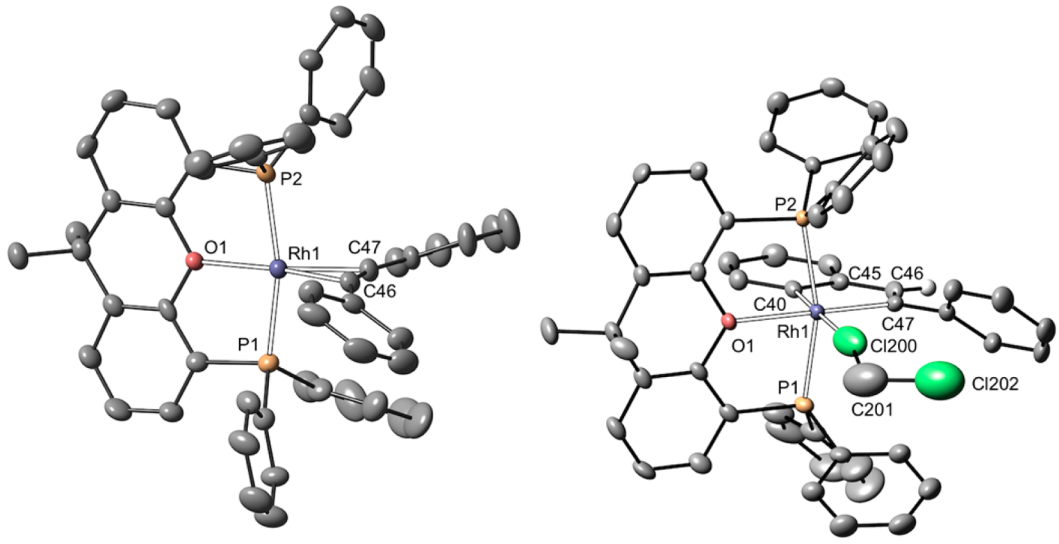

Figure 4. Solid-state structure of complexes **6** (left) and **7** (right) showing the cations only. Displacement ellipsoids are shown at the 50% probability level. Most hydrogen atoms are not shown. Selected bond lengths (Å) and angles (deg): (**6**)**:** Rh1−P1, 2.2825(12); Rh1−P2, 2.2896(12); Rh1−C46, 2.114(4); Rh1−C47, 2.094(4); Rh1−O1, 2.138(3); C46−C47, 1.256(6); P1−Rh1−P2, 166.65(4); O1−Rh1−C46, 166.73(15); O1−Rh1−C47, 158.46(15). (**7**)**:** Rh1−P1, 2.3036(11); Rh1−P2, 2.2969(10); Rh1−C40, 2.010(4); Rh1−C47, 2.020(4); Rh1−O1, 2.223(3); C45−C56, 1.447(7); C46−47, 1.348(7); Rh1−Cl200, 2.393(7); Cl200−C201, 1.788(7); C201−Cl202, 1.781(7); P1−Rh1−P2, 163.83(4); O1−Rh1−C40, 94.81(14); O1−Rh1−C47, 176.11(15). Only the major disordered competent of the CH_2Cl_2 ligand is shown.

plexes with Xantphos−^{t}Bu[11] or Xantphos−^{i}Pr[12] are soluble in benzene and shown to be monomers in the solid state. This presumably reflects the differing steric demands of the P-substituents. Suspension of complex **4** in toluene and addition of H_2 resulted in the formation of the neutral, soluble, Rh(III) *cis*-dihydride complex Rh(κ^3-$_{P,O,P}$-Xantphos)$(H)_2$Cl, **5**, obtained in 79% yield (Scheme 3) as colorless crystals. The solid-state structure of **5** is shown in Figure 3 and is very closely related to recently reported Rh−Xantphos−^{t}Bu[11] and Ir−Xantphos−^{i}Pr[12] analogues (i.e., **B** Figure 2). The NMR spectroscopic data for **5** are in full accord with the solid-state structure and show inequivalent hydride environments in the ^{1}H NMR spectrum, in contrast to complex **3**. The formation of **5** in good yield from simple addition of H_2 to **4** further supports the latter's formulation.

Removal of the chloride ligand in **4** is easily achieved by treatment of a suspension in 1,2-$C_6H_4F_2$ solvent with Na[BAr^F_4] in the presence of a slight excess of diphenylactylene to yield the Rh(I) complex *mer*-[Rh(κ^3-$_{P,O,P}$-Xantphos)(η^2-PhCCPh)][BAr^F_4], **6**, as orange crystalline material in good (82%) yield on work-up. The solid-state structure of the cation in complex **6** is shown in Figure 4, and this shows the alkyne to be bound perpendicular to the Rh−POP plane (angle between planes = 90.7°). The C−C distance [1.256(6) Å] is lengthened compared to free ligand [1.206(2) Å[29]]. The NMR spectroscopic and microanalytical data support this formulation; for example, a single environment is observed at δ 20.4 [d, J(RhP) = 124 Hz] in the ^{31}P{^{1}H} NMR spectrum, while one, relative integral 6 H, signal is observed for the Xantphos methyl groups. There are surprisingly few pseudo square planar complexes reported which have pincer ligands and bound alkynes or alkenes. One example is (PCP)Ir(*trans*-1,4-phenyl-but-3-ene-1-yne) [PCP = (κ^3-C_6H_3-2,6-$(CH_2P^tBu_2)_2$)], which also adopts a similar coordination mode with the metal−pincer fragment to **6** and shows a similar C−C distance [1.270(4) Å].[30] Complex **6** represents an excellent starting point into the C−S activation chemistry, which is described in the next section.

An alternative methodology for generating complex **6** is addition of H_2 (1 atm) to complex **1a** in CH_2Cl_2 solution to form complex **2a**, evacuation, followed by addition of a CH_2Cl_2 solution of diphenylacetylene (Scheme 5). Under these conditions of excess alkyne, *cis*-stilbene is also observed to be formed by ^{1}H NMR spectroscopy [δ 6.57]. Also produced is a parallel product, identified by NMR spectroscopy and single crystal X-ray diffraction as [Rh(κ^3-$_{P,O,P}$-Xantphos)(ClCH$_2$Cl)-(σ,σ-(C_6H_4)C(H)=CPh)][BAr^F_4], **7**. Complex **7** is formed as a major product relative to **6** under these conditions (relative ratio 2:1 of **7** to **6**). Although single crystals of complex **7** could be produced in this manner, in bulk form it was always contaminated with some **6**.

The solid-state structure of **7** (Figure 4) shows a *trans*-stilbene-derived ligand that has additionally undergone C−H activation to give a metallacyclopentadiene [Rh−C 2.010(4) and 2.020(4) Å]. Similar activation of diphenylactylene has been reported at Rh and Ir centers,[31,32] and the structural metrics previously reported for these metallacyclopentadienes are similar to **7**. The coordination sphere of the metal is completed by a coordinated CH_2Cl_2 ligand [Rh−Cl, 2.393(7) Å]. Complexes in which CH_2Cl_2 acts as ligand are now well−established,[33] and a handful of examples with Rh have been reported.[34−37] The ^{1}H and ^{31}P{^{1}H} NMR data for complex **7** (CD_2Cl_2 solution) are in full accord with the solid-state structure. In particular, the ^{1}H NMR spectrum shows inequivalent Xantphos methyl groups, and signals that can be attributed to the metallocycle unit. Signals due to the coordinated CH_2Cl_2 ligand were not observed, but it is likely that this ligand is in rapid exchange with the bulk solvent.[33] The ^{31}P{^{1}H} NMR spectrum displays a single environment as a doublet, showing coupling to ^{103}Rh consistent with coordination with a Rh(III) center [J(RhP) = 119 Hz] and a mirror−plane of symmetry in solution.

DOI: 10.1021/om500984y
Organometallics 2015, 34, 711−723

The observation that complex **7** is preferentially formed over complex **6** when complex **2a** is formed *in situ* suggests that this latter Rh(III) complex is central to the C−H activation process to form **7**. Complex **6** does not undergo C−H activation to form **7** (Scheme 4), supporting this hypothesis. The C−H activation process can be reversed. Complex **7** reacts with H_2 (1 atm) *slowly* (12 h, CD_2Cl_2) to form complex **2a** as determined by $^{31}P\{^1H\}$ NMR spectroscopy. No *cis*-stilbene was observed to be formed [δ 6.57, $CDCl_3$] under these conditions, and when the reaction was performed with D_2, signals at δ 7.25 and 7.57 were observed in the ^2H NMR spectrum, consistent with formation of *trans*-PhCH=C(D)(C_6H_4D) [lit. ^1H δ 7.19, 7.60 $CDCl_3$[38]]. d_2-**2a** was also observed to be formed by a broad signal at ~δ −18 in the ^2H NMR spectrum. This shows that under conditions exogenous of H_2, complex **7** can be recycled back to form **2a**, but only slowly.

Scheme 4. Reactivity of Complex 7[a]

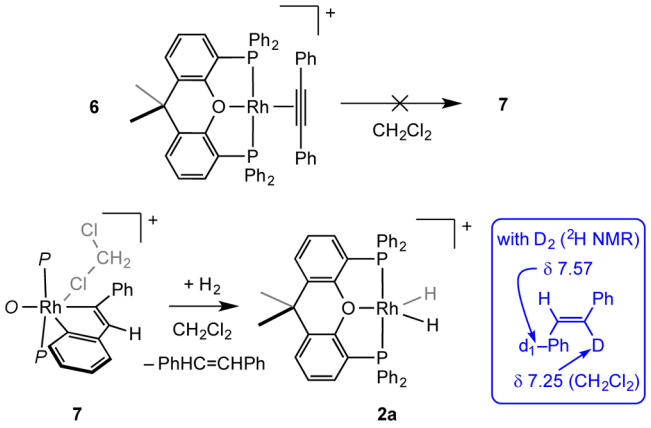

[a] $[BAr^F_4]^-$ anions are not shown.

Scheme 5. Suggested Mechanism for the Formation of Complex 7[a].

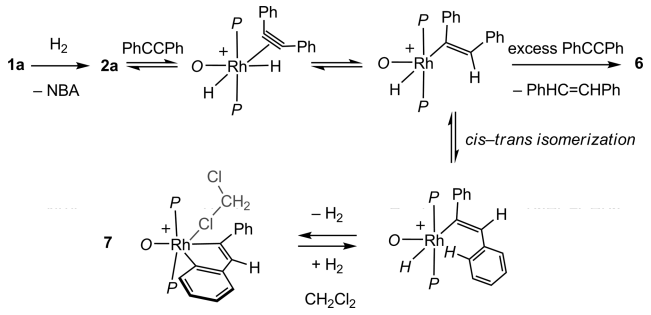

[a] $[BAr^F_4]^-$ anions are not shown. Xantphos is abbreviated POP.

A suggested mechanism for the formation of complex **7** is shown in Scheme 5. Addition of H_2 to **1a** forms the dihydride complex **2a**, which then undergoes coordination and hydride insertion with diphenylacetylene to give the corresponding *cis*-diphenylvinyl intermediate. The pathway then bifurcates: Elimination of *cis*-stilbene (observed) and subsequent coordination of diphenylacetylene eventually give **6**. Alternatively a *cis*−*trans* isomerization (possibly via a metallacyclopropene intermediate)[31,39] followed by C−H activation at the *ortho*-position of arene occurs, likely via a sigma−CAM process (sigma−complex assisted metathesis),[40] loss of H_2, and coordination of CH_2Cl_2 to form **7**.

2.2. C−S Activation Chemistry. With a suitable Rh(I) precursor to C−S activation in hand in complex **6**, reactivity with a variety of arylsulfides was explored (Figure 5). Given the use of the substrate **I** [2-(methylthio)acetophenone] in our recently reported carbothiolation chemistry,[19,20] initial studies focused upon using this starting material. Addition of **I** to a toluene solution of **6** resulted, at 298 K, in the formation of a mixture of two isomers, identified spectroscopically as *fac*- and *mer*-[Rh(κ^3-$_{P,O,P}$-Xantphos)(σ,κ^1-C_6H_4COMe)(SMe)][BAr^F_4], **8**, Scheme 6. These isomers were initially formed in a 20:1 ratio respectively after 20 min and equilibrated over time to give κ^3-*mer*-**8** as the thermodynamic product after 32 h. This process may be accelerated by heating to 373 K for 40 min, after which time κ^3-*mer*-**8** can be isolated in good (70%) yield as the only product. In both cases free diphenylacetylene is also observed to be formed. The $^{31}P\{^1H\}$ NMR spectrum of κ^3-*fac*-**8** shows two environments, each with a distinctive doublet of doublet coupling pattern, that show two very different magnitudes of coupling to ^{103}Rh: δ 34.8 [J(RhP) = 150, J(PP) = 17 Hz] and δ 22.6 [J(RhP) = 104, J(PP) = 17 Hz]. Such a pattern is characteristic of ^{31}P environments in which one sits opposite to a high *trans* influence ligand (such a SMe) while one sits opposite a weaker ligand, i.e. the ketone.[39,41] The ^1H NMR spectrum shows two signals at δ 1.56 and 1.43 (both of relative integral 3 H) as doublets [J = 7.6 and 1.2 Hz, respectively]. These are assigned to the SMe and ketone−methyl group, respectively, and the larger coupling to ^{31}P in the former (confirmed by selective decoupling experiments) is fully consistent with its *trans* disposition to a phosphine.[20,39] Although we have not obtained a solid-state structure for κ^3-*fac*-**8**, similar complexes have been crystallographically characterized with DPEphos.[10,39,41] The NMR data for κ^3-*mer*-**8** are also fully consistent with its formulation; notably, a single environment is observed in the $^{31}P\{^1H\}$ NMR spectrum [J(RhP) = 106 Hz], and the SMe [δ 0.87] and ketone−methyl groups [δ 1.99] are observed as singlets in the ^1H NMR spectrum; consistent with their now *cis*-relationship with the phosphines. Two methyl environments are observed for the Xantphos ligand. The solid-state structure of κ^3-*mer*-**8** is shown in Figure 6. In the unit cell there are two crystallographically distinct cations, for which the structural metrics are very similar. The structure demonstrates the κ^3-*mer* geometry of the final product, in which the thiomethyl and aryl groups sit mutually

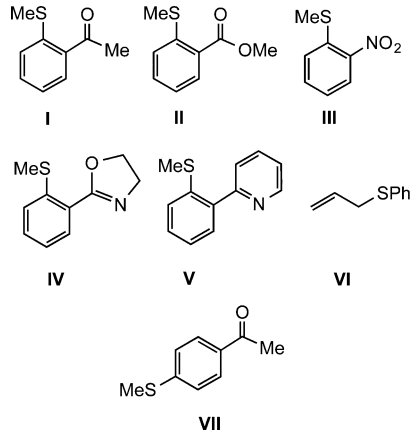

Figure 5. Arylsulfides used in this study.

DOI: 10.1021/om500984y
Organometallics 2015, 34, 711−723

Scheme 6. Formation of *fac*-8 and *mer*-8[a]

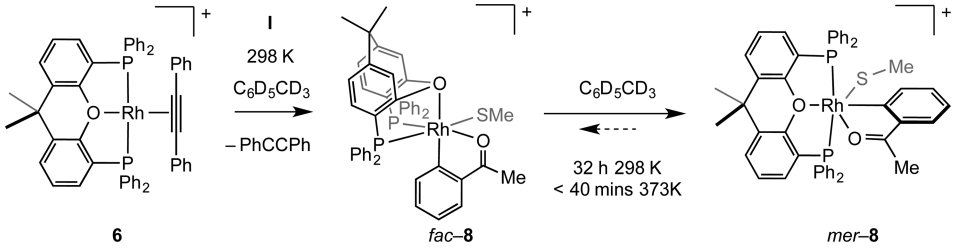

[a] $[BAr^F_4]^-$ anions are not shown.

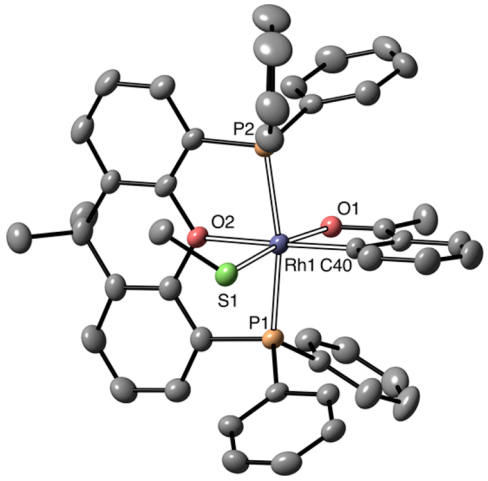

Figure 6. Solid-state structure of complex *mer*-**8** showing the cation only. Only one of the crystallographically independent cations is shown. Displacement ellipsoids are shown at the 50% probability level. Hydrogen atoms are not shown. Selected bond lengths (Å) and angles (deg): Rh1–P1, 2.2983(16); Rh1–P2, 2.3068(16); Rh1–O1, 2.102(3); Rh1–O2, 2.215(3); Rh1–S1, 2.3373(14); Rh1–C40, 1.975(5); P1–Rh–P2, 165.22(5); O1–Rh1–P1, 90.08(10); O1–Rh1–S1, 173.00(10).

cis with one another [Rh1–C40, 1.975(5); Rh1–S1, 2.3373(14) Å]. The remaining coordination site on the Rh(III) center is occupied by a dative bond from the *ortho* substituent on the arene [Rh1–O1, 2.102(3) Å]. The thiomethyl group sits *syn* to one phosphine and *anti* to the other, and it is likely that low energy libration around the Rh–S bond gives the cation time-averaged C_s symmetry in solution.

Exchange between isomers of Xantphos, in which the phosphines adopt a *cis* or *trans* geometry, has been noted previously, and in some cases this is reversible.[10,42,43] For the system *fac*/*mer*-[Rh(κ^3-$_{P,O,P}$-Xantphos)($PCyp_3$)(H_2)][BAr^F_4], equilibrium measurements indicate that the *fac* isomer is preferred and that although enthalpically there is little difference between the isomers, entropic considerations determine the final position of the equilibrium (ΔS is positive for the generation of the *fac* isomer).[10] On heating *mer*-**8** (373 K, $C_6D_5CD_3$), we saw no evidence, to the detection limit of ^{31}P NMR spectroscopy, for *fac*-**8**. However, we cannot discount its formation at a very low equilibrium concentration under these conditions.

Using the protocol for the isolation of pure C–S activated product developed above, the 2-arylmethylsulfides **II**–**V** were combined with complex **6** to afford complexes **9**–**12** in good yields (66%–78%), all as the *mer*-isomers, Scheme 7. These red/brown complexes have been characterized by NMR

Scheme 7. Products of Reaction with the 2-Arylmethylsulfides Used in This Study[a,b]

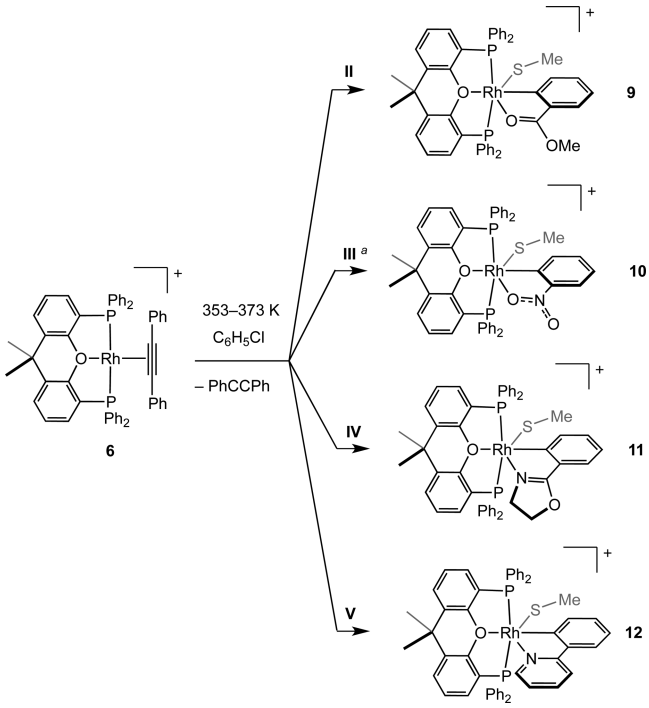

[a] CH_2Cl_2 at 298 K. [b] $[BAr^F_4]^-$ anions are not shown.

spectroscopy, ESI–MS, microanalysis, and X-ray crystallography (apart from complex **9**, in which extensive disorder of the cation precluded a reliable analysis). Solid-state structures of the cations in complexes **10** and **11** are shown in Figure 7 (complex **12** is presented in the Supporting Materials) and are closely related to that of *mer*-**8**. For the structures **10**–**12**, the activated thio–aryl ligand is equally disordered between two orientations in which the SMe and *ortho*-coordinating groups have swapped positions, giving the overlaid disordered structures C_{2v} symmetry in the solid state. Although this disorder could be modeled satisfactorily, this does mean that caution should be exercised in the interpretation of the fine details of the structural metrics around the metal. Nevertheless, the structures confirm the formulation.

When allyl phenyl sulfide **VI** is combined with complex **6**, the C–S activated product *fac*-[Rh(κ^3-$_{P,O,P}$-Xantphos)(η^3-C_3H_5)(SPh)][BAr^F_4], **13**, is isolated as a green crystalline solid in 60% yield, Scheme 8. The solid-state structure of **13** is shown in Figure 8 and demonstrates the κ^3-*fac* geometry of the Xantphos ligand [Rh1–O1, 2.200(2) Å, P–Rh–P 109.54(3)°] and the η^3 coordination mode of the allyl group at the Rh(III)

DOI: 10.1021/om500984y
Organometallics 2015, 34, 711–723

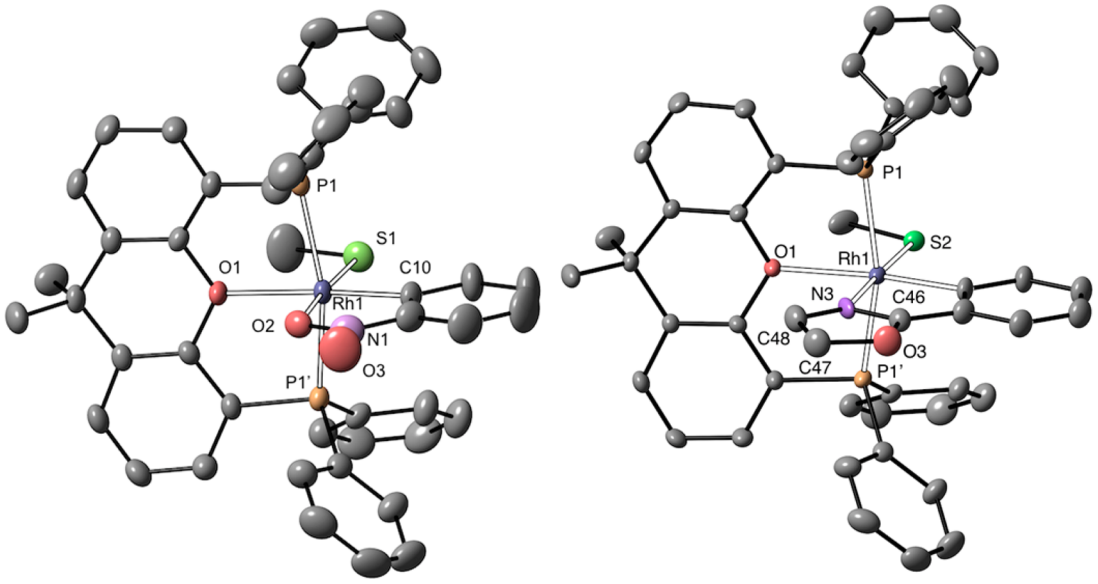

Figure 7. Solid-state structure of complexes **10** (left) and **11** (right) showing the cations only. Only one disordered component of each is shown. Displacement ellipsoids are shown at the 50% probability level. Hydrogen atoms are not shown. Selected bond lengths (Å) and angles (deg): **(10):** Rh1−P1, 2.3143(7); Rh1−O1, 2.200(2); Rh1−O2, 2.133(3); Rh1−S1, 2.3074(10); Rh1−C10, 1.967(4); P1−Rh−P1′, 165.07(3); O1−Rh1−P1, 82.690(17); O2−Rh1−S1, 175.13(8). **(11):** Rh1−P1, 2.3060(9); Rh1−O1, 2.209(4); Rh1−N3, 2.173(5); Rh1−S2, 2.296(4); N3−C48, 1.397(7); C48−C47, 1.441(6); C47−O3, 1.463(7); O3−C46, 1.339(6); C46−N3, 1.323(5); P1−Rh−P1′, 165.42(5); O1−Rh1−P1, 82.72(2); N3−Rh1−S1, 177.54(18).

Scheme 8. Synthesis of Complexes 13 and 14[a]

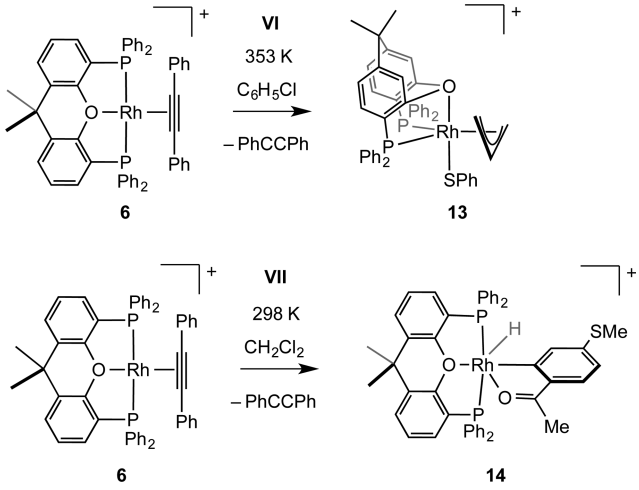

[a] $[BAr^F_4]^-$ anions are not shown.

center. The molecule has, noncrystallographically imposed, pseudomirror symmetry. The solution NMR data for **13** are consistent with this, with one ^{31}P environment observed [J(RhP) = 132 Hz], while the allyl ligand is revealed by three signals in a 1:2:2 ratio [multiplets centered at δ 4.80, 3.99, 2.64]. Oxidative addition of allyl sulfides to late transition metals is known.[44,45] Presumably this process occurs via initial coordination of the alkene followed by oxidative cleavage of the C−S bond.[44] Very few examples of crystallographically characterized Xantphos (or DPEphos) complexes that also contain allyl ligands have been reported, and all have a κ^2-P,P geometry of the chelate ligand,[46] different from the κ^3-POP observed for complex **13**.

The reaction of (4−methylthio)acetophenone **VII** with complex **6** probes the requirement for a *ortho*-directing group in these C−S activations, Scheme 8. The product of this reaction is *mer*-[Rh(κ^3-$_{P,O,P}$−Xantphos)(σ,κ^1-C_6H_3(COMe)-SMe)(H)][BAr^F_4], **14**, isolated in moderate yield (38%) as colorless crystalline material, for which NMR spectroscopy and a single crystal X-ray diffraction study showed it to be the product of C−H activation *ortho* to the directing ketone group. The ^1H NMR data for **14** show a single hydride environment at δ −14.99 (relative integral 1 H) as a doublet of triplets and the absence of a methyl resonance below δ 1 that would be indicative of a Rh−S*Me* group. The $^{31}P\{^1H\}$ NMR spectrum displays a single environment showing coupling to a Rh(III) center [δ 39.5, J(RhP) = 114 Hz]. These data suggest C−H activation has occurred rather than C−S activation, and the solid-state structure derived from a single crystal X-ray analysis confirms this, Figure 8. This shows that the 4-(methylthio)-acetophenone has undergone C−H activation *ortho* to the ketone to afford a *cis*-hydridoaryl motif, with the hydride ligand located in the final Fourier difference map. The rhodium's coordination sphere is completed by coordination of the ketone through a dative bond, similar to that observed for the C−S activated products. Such reactivity is directly related to the directed activation of *ortho*-C−H bonds first reported by Murai,[47] in which arylketones underdo hydroarylation with alkenes.[48] Complex **14** does not react further with alkynes, for example phenyl acetylene.

2.3. Alkyne Trimerization. Complex **6** does not react further with diphenylacetylene. However, it does react slowly (20 h, 298 K) with phenylacetylene to afford the products of cyclotrimerization, 1,2,3-$Ph_2C_6H_3$ and 1,2,4-$Ph_3C_6H_3$, as identified by ^1H NMR spectroscopy and GC−MS. These are formed in a 2:1 ratio (Scheme 9). Complex *mer*-**8** will also promote this process, but only at elevated (373 K) temperature, and there is no reaction at 298 K. This latter reaction presumably occurs via initial carbothiolation to release the alkenyl sulfide product (observed by ^1H NMR spectroscopy), and the resulting [Rh(Xantphos)]$^+$ fragment is then free to

DOI: 10.1021/om500984y
Organometallics 2015, 34, 711−723

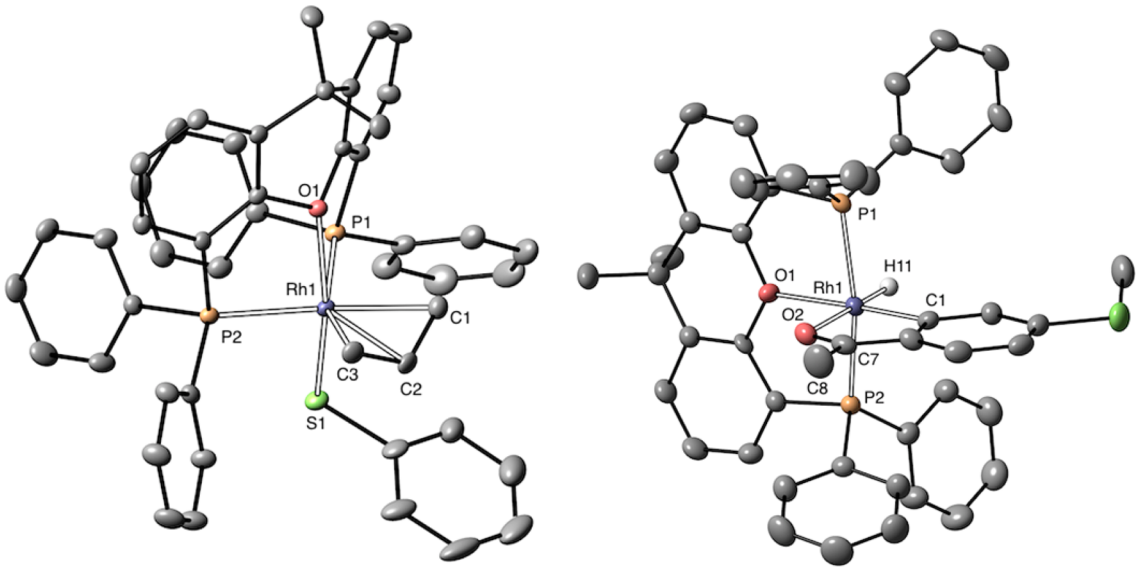

Figure 8. Solid-state structure of complexes **13** (left) and **14** (right) showing the cations only. Displacement ellipsoids are shown at the 50% probability level. Most hydrogen atoms are not shown. Selected bond lengths (Å) and angles (deg), **(13):** Rh1−P1, 2.2847(7); Rh1−P2, 2.3337(7); Rh1−O1, 2.200(2); Rh1−S1, 2.3393(8); Rh1−C1, 2.190(3); Rh1−C2, 2.197(3); Rh1−C3, 2.249(3); C1−C2, 1.408(5); C2−C3, 1.388(5); P1−Rh1−P2, 109.54(3); O1−Rh1−S1 166.44(6). **(14):** Rh1−P1, 2.2699(6); Rh1−P2, 2.2729(6); Rh1−O1, 2.1861(17); Rh1−O2, 2.1609(18); Rh1−C1, 1.968(3); P1−Rh1−P2, 166.45(2); O1−Rh1−P1, 83.53(5); O1−Rh1−C1, 175.74(9).

Scheme 9. Phenyl Acetylene Trimerization As Catalyzed by Complexes 6 and *mer*-8

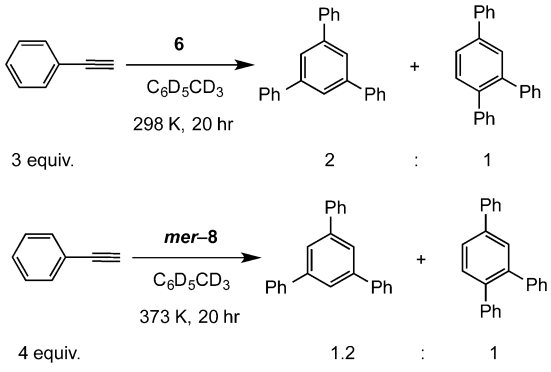

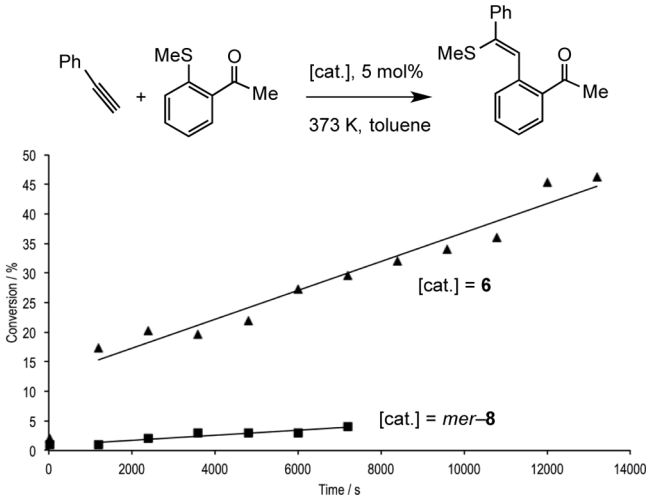

Figure 9. Time conversion plot for the catalytic reaction of **I** (0.1 M) and phenylactylene (0.2 M). [cat.] = **6** or *mer*-**8** 0.005 M, solvent = $C_6D_5CD_3$, Temperature = 373 K. Both reactions reach completion. Lines of best fit are for visual comparison only.

mediate cyclotrimerization. These trimerization products are also observed during carbothiolation catalysis but in low relative yield (less than 20%), meaning that although this process is competitive with carbothiolation in this system, use of a slight excess of alkyne (2 equiv) means that full conversion of the ketone is achieved.

2.4. Catalysis. Under room temperature conditions (298 K) complex **6** will only slowly catalyze the carbothiolation of **I** with phenyl acetylene (55% conversion at 24 h). However, heating to 373 K results in faster turnover (6 h) with full conversion to the alkenyl sulfide product. Complex *mer*-**8** was the only observed organometallic product during this catalysis [by $^{31}P\{^1H\}$ NMR spectroscopy]. Starting from *mer*-**8**, the reaction is considerably slower (16 h, 373 K), and again, *mer*-**8** is the only observed species during catalysis. Following these reactions by *in situ* NMR spectroscopy during the early stages of catalysis using 1,3-dimethoxybenzene as internal standard (Figure 9) revealed the temporal profiles for the formation of the product for both starting pre-catalysts. For catalysts using complex **6**, initial very rapid catalysis (~15% conversion after 20 min) is then followed by a much slower rate. These data are consistent with the initial formation of a very active catalyst that turns over the carbothiolation rapidly but quickly forms a less active catalyst. We suggest, based on our stoichiometric experiments, that this can be explained by the initial formation of *fac*-**8**. In principle this could decoordinate its POP ether linkage relatively easily to allow access to the alkyne to the now 16-electron metal center. Such potentially hemilabile behavior has been noted for related Xantphos complexes on reaction with MeCN.[10] Isomerization to the presumably less active *mer*-**8**, shown to be rapid at 373 K, results in a slower rate of catalysis. Consistent with this, *mer*-**8** is the only observed organometallic species during catalysis, as the resting state, while starting from *mer*-**8** results in no rapid initial burst of activity, but only slow turnover at a rate broadly similar to that for the slow regime when starting from **6**. Whether catalysis in

DOI: 10.1021/om500984y
Organometallics 2015, 34, 711−723

the slow regime occurs by a small (undetectable by ^{31}P NMR spectroscopy) equilibrium concentration of *fac*-**8** or an alternative active species is not clear. A suggested pathway for catalysis is shown in Scheme 10. This has close similarities for

Scheme 10. Suggested Catalytic Cycle for the Homogenous Carbothiolation Catalysis Using the [Rh(Xantphos)]$^+$ Catalyst

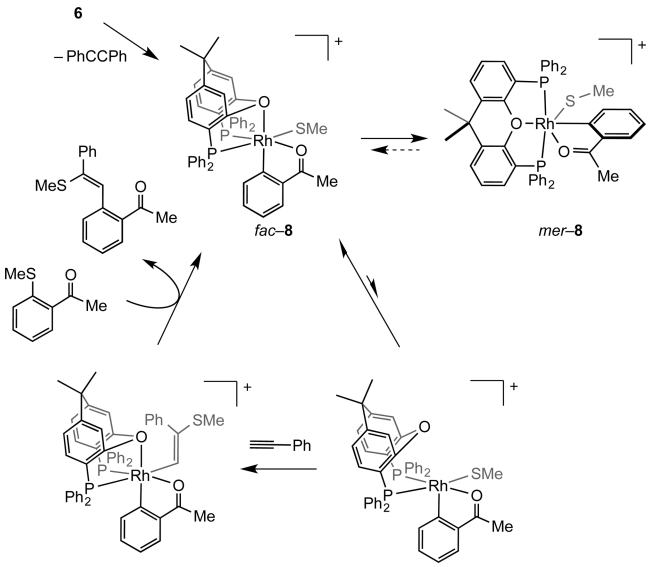

those suggested for alkyne carbothiolation[20] and alkyne hydroacylation[39] using the [Rh(DPEphos)]$^+$ system. We have observed related intermediates previously in alkyne hydroacylation systems with [Rh(DPEphos)]$^+$ fragments.[39,41]

Given the scatter present in the data (Figure 9), we are reluctant to speculate further the likely rate-determining steps or the order of reaction, and although the broad temporal profile was reproducible (e.g., *mer*-**8** versus **6**), there was significant variation between repeat runs with regard to the approximate rate in the slow regime. Tests for homogeneous/heterogeneous behavior indicated a homogeneous catalyst[49] (Hg-test, sub-stoichiometric phosphine, microfiltration tests; a clear red solution is observed during catalysis). However, we cannot completely rule out the presence of a small amount of colloidal Rh-catalyst, or decomposition to a different active species. Notably the Hg-test still showed an initial burst of reaction rate followed by slower turnover, consistent with our mechanistic hypothesis. It is also interesting to note that when catalysis is performed in dichloroethane solvent at 353 K (rather than toluene at 373 K), a very different profile is observed characteristic of a greater than zero order process: the reactions are much faster *and* the reaction solutions are observed to be black.[19] Whether this indicates a change from homogeneous to heterogeneous catalysis under these different conditions is as yet unclear, but it is notable that nanoparticle formation has been shown to be strongly dependent on solvent polarity.[50,51]

3. CONCLUSIONS

We report the synthesis of *mer*-[Rh(κ^3-$_{P,O,P}$-Xantphos)(η^2-PhCCPh)][BAr$^F_4$], **6**, which acts as a latent source of the [Rh(κ^3-$_{P,O,P}$-Xantphos)]$^+$ fragment. That this complex comes from simple halide abstraction from [Rh(κ^3-$_{P,O,P}$-Xantphos)Cl]$_n$ suggests that this might well be a useful methodology for future synthetic and catalytic studies. Demonstrating the utility of **6** in this regard, we have shown that it readily undergoes ketone-directed C–S and C–H activation processes with aryl–ketosulfides. Additionally we have also reported rare examples of Rh–chlorobenzene and Rh–dichloromethane complexes. The temporal evolution of catalysis using **6** shows initial fast catalysis and then and then much slower turnover, and we suggest that the *fac*-isomer of the C–S activation product (i.e., *fac*-**8**) is considerably more active than the *mer*-isomer (i.e., *mer*-**8**), the latter being formed rapidly by isomerization. A future strategy for optimizing this catalyzed carbothiolation reaction might well be to limit the flexibility of the ligand set so that this isomerization does not occur, and studies are currently ongoing to study the effect of incorporating such ligands into the catalyst structure.

4. EXPERIMENTAL SECTION

General Experimental Procedures. All manipulations, unless otherwise stated, were performed under an argon atmosphere using standard Schlenk and glovebox techniques. Glassware was oven-dried at 130 °C overnight and flamed under vacuum prior to use. Pentane, dichloromethane, benzene, and toluene were dried using a Grubbs type solvent purification system (MBraun SPS-800) and degassed by successive freeze–pump–thaw cycles.[52] Benzene, toluene, C_6H_5F, and 1,2-$F_2C_6H_4$ were, where appropriate, further dried over CaH_2, vacuum distilled, and stored over 3 Å molecular sieves. Chlorobenzene (less than 0.005 H_2O) was purchased from Aldrich and degassed by successive freeze–pump–thaw cycles and stored over 3 Å molecular sieves. Na[BAr$^F_4$],[53] [Rh(COE)$_2$Cl]$_2$,[54] [Rh(NBD)Cl]$_2$,[55] [Rh(κ^2-$_{P,P}$-Xantphos)(NBD)][BAr$^F_4$] (**1a**),[15] (9,9-dimethyl-9H-xanthene-4,5-diyl)bis(3,5-bis(trifluoromethyl)phenyl)phosphine,[56] 2-(methylthio)-acetophenone,[20] 4-(methylthio)acetophenone,[20] 2-(2-(methylthio)-phenyl)-4,5-dihydrooxazole,[57] and 2-(2-(methylthio)phenyl)-pyridine[58] were prepared by literature methods. NMR spectra were recorded on a Bruker Avance III HD nanobay 400 MHz (Hg400) and Bruker DPX200 spectrometer at room temperature, unless otherwise stated. ^1H NMR spectra are referenced to residual solvent signals. ^{31}P NMR spectra were referenced against 85% H_3PO_4 (external). Chemical shifts (δ) are quoted in ppm and coupling constants (J) in Hz. ESI-MS were recorded on a Bruker micrOTOF instrument interfaced with a glovebox.[59] Microanalysis was performed at London Metropolitan University. Reverse phase HPLC analysis was performed on a Ascentis Express C18, 2.7 μm column (4.6 mm × 100 mm), eluted by gradient MeCM/H_2O. GC-MS was performed on a Waters GCT ToF mass spectrometer.

Synthesis of 2-Nitrothioanisole. To a stirred solution of 1-fluoro-2-nitrobenzene (0.268 mg, 1.9 mmol) in DMF (10 mL) was added a sodium thiomethoxide 21% aqueous solution (2.2 mmol). After the addition was complete, the solution was stirred at room temperature for 2 days. Then 100 mL H_2O was added to precipitate the product. The solvent was decanted off and the resulting solid was recrystallized (dichloromethane/petrol) to give the sulfide as pure product (167 mg, 52%). The ^1H NMR data is consistent with the reported values.[60]

^1H NMR (200 MHz, CDCl$_3$). δ 8.26 (dd, J = 8.2 Hz, J = 1.4 Hz, 1H), 7.59 (ddd, J = 8.2 Hz, J = 7.0 Hz, J = 1.4 Hz, 1H), 7.37 (d, J = 7.6 Hz, 1H), 7.25 (ddd, J = 8.2 Hz, J = 7.2 Hz, J = 1.4 Hz 1H), 2.50 (s, 3H).

Synthesis of New Complexes: *cis*-[Rh(κ^2-$_{P,P}$-Xantphos-3,5-C$_6$H$_3$(CF$_3$)$_2$)(NBD)][BAr$^F_4$] (1b). Xantphos-3,5-$C_6H_3(CF_3)_2$ (243 mg, 0.217 mmol) in CH_2Cl_2 (13 mL) was added dropwise to [Rh(NBD)Cl]$_2$ (50 mg, 0.108 mmol) in CH_2Cl_2 (1 mL). The resulting reaction mixture was then added dropwise to Na[BAr$^F_4$] (192 mg, 0.217 mmol) in CH_2Cl_2 (1 mL) and the mixture was stirred for 2 h. The solution was filtered, and the filtrate solvent was reduced to ~5 mL. Then the solution was layered with pentane (20 mL). The solution was stored overnight at −18 °C to give the recrystallization product. Yield = 80%, 378 mg.

DOI: 10.1021/om500984y
Organometallics 2015, 34, 711–723

^{1}H NMR (400 MHz, CD_2Cl_2). δ 8.01−7.97 (m, 4H, Ar−H), 7.91 (d, *J* = 7.6 Hz, 2H, Ar−H), 7.76−7.69 (m, 8H, BAr^F_4), 7.64−7.54 (m, 8H, Ar−H), 7.54 (s, 4H, BAr^F_4), 7.47 (t, *J* = 8.0 Hz, 2H, Ar−H), 6.98−6.92 (m, 2H, Ar−H), 4.04 (s, 4H, NBD CH═CH), 3.79 (s, 2H, NBD CH), 1.87 (s, 6H, Xantphos Me), 1.48 (s, 2H, NBD CH_2).

$^{31}P\{^1H\}$ NMR (160 MHz, CD_2Cl_2). δ 17.5 [d, $^1J_{RhP}$ = 148 Hz].

ESI-MS (Acetone) Positive Ion. $[M]^+$ *m*/*z* = 1317.06 (calc. 1317.06).

Microanalysis. $C_{86}H_{44}BF_{48}OP_2Rh$ (2180.88) requires: C 47.36, H 2.03; found: C 47.50, H 1.95.

[Rh(κ^3-$_{P,O,P}$-Xantphos)(H)$_2$][BAr^F_4] (2a). The title compound was prepared in situ by placing a solution of [Rh(κ^2-$_{P,P}$-Xantphos)(NBD)][BAr^F_4] (10 mg, 6.1 × 10^{-6} mol) in CD_2Cl_2 (0.3 mL) under 4 atm of hydrogen. The compound was characterized *in situ* by NMR spectroscopy and ESI-MS. There was no change to the NMR spectrum on removal of the solvent to dryness and redissolving in CD_2Cl_2.

^{1}H NMR (300 MHz, CD_2Cl_2). δ 7.84−7.38 [m, 38H, Ar−H + BAr^F_4; 7.72 (8H, BAr^F_4), 7.55 (4H, BAr^F_4), 1.73 (br s, 6H, CH_3), −18.28 (dt, 2H, *J*(RhH) = 33, *J*(PH) = 12, Rh−H).

$^{31}P\{^1H\}$ NMR (122 MHz, CD_2Cl_2). δ 41.50 (d, *J*(RhP) = 117).

ESI-MS (fluorobenzene, 60 °C, 4.5 kV) positive ion. $[M]^+$ *m*/*z* = 683.1250 (calc. 683.1134).

***mer*-[Rh(κ^3-$_{P,O,P}$-Xantphos-3,5-$C_6H_3(CF_3)_2$)(H)$_2$(κ^1-ClC_6H_5)][BAr^F_4] (2b/3).** **1b** (50 mg, 0.023 mmol) was dissolved in chlorobenzene (5 mL), then the solution was degassed and reacted with hydrogen for 30 min under 4 atm. Then the solution was degassed again and layered with hexane (10 mL). The solution was stored overnight at −18 °C to give white solid. Yield = 79%, 40 mg. Crystals of **3** suitable for X-ray diffraction were obtained from chlorobenzene solution *in situ*.

^{1}H NMR (400 MHz, CD_2Cl_2). δ 8.21 (s, 4H), 8.10−7.98 (br, 5H, C_6H_5Cl), 7.96 (dd, *J* = 7.6 Hz, *J* = 1.2 Hz, 2H), 7.74−7.66 (m, 8H, BAr^F_4), 7.62 (t, *J* = 7.6 Hz, 2H), 7.53 (s, 4H, BAr^F_4), 7.50−7.42 (m, 2H), 7.37−7.22 (m, 8H), 1.80 (s, 6H, Xantphos Me), −17.89 (br. s, 2H).

$^{31}P\{^1H\}$ NMR (160 MHz, CD_2Cl_2). δ 44.0 [d, $^1J_{RhP}$ = 119 Hz].

The following NMR spectroscopic data in C_6D_5Cl was obtained by placing a solution of **1b** (8 mg) in D-chlorobenzene (0.4 mL) under 4 atm of hydrogen, and characterized in situ by NMR spectroscopy.

^{1}H NMR (500 MHz, C_6D_5Cl). δ 8.23−8.17 (m, 8H, BAr^F_4), 8.15−8.00 (m, 8H), 7.85 (s, 4H), 7.56 (s, 4H, BAr^F_4), 7.43−7.40 (m, 2H), 7.38−7.32 (m, 2H), 7.09 (t, *J* = 7.5 Hz, 2H), 1.33 (s, 6H, Xantphos Me), −17.74 (br. s, 2H). (coordinated D-chlorobenzene is not observed).

$^{31}P\{^1H\}$ NMR (200 MHz, C_6D_5Cl). δ 45.3 [d, $^1J_{RhP}$ = 118 Hz].

The $^{31}P\{1H\}$ and ^1H NMR spectra of the product in CH_2Cl_2 at 183 K are essentially unchanged from that in CD_2Cl_2 at 298 K.

Microanalysis. $C_{85}H_{43}BClF_{48}OP_2Rh$ (2180.88) requires: C 46.34, H 1.97; found: C 46.47, H 1.91.

[Rh(Xantphos)Cl]$_n$ (4). To a J. Youngs tube containing [Rh(COE)$_2$Cl]$_2$ (305 mg, 0.425 mmol) and Xantphos (492 mg, 0.85 mmol) was added 10 mL benzene, sealed, and heated to 80 °C for 4 h. The solution changed color to dark red, followed by product precipitation. The resulting precipitate was filtered and washed with pentane. The precipitate was dried under vacuum to yield a brick-red powder. Yield = 91%, 555 mg. Complex **4** was insoluble in benzene, acetone, and reacts with dichloromethane to give an unidentified mixture. Toluene can be replaced for benzene in the procedure with no significant change in yield.

Microanalysis. $C_{39}H_{32}ClOP_2Rh$ requires: C 65.33, H 4.50; found: C 65.41, H 4.37.

***mer*-[Rh(κ^3-$_{P,O,P}$-Xantphos)(H)$_2$Cl] (5).** The title compound was formed by placing a solution of **4** (50 mg, 7.0 × 10^{-2} mmol) in toluene (5 mL) under an atmosphere of H_2 (1 atm). The solution was stirred for 16 h at room temperature. The solution was degassed and was reduced to ∼1 mL, 10 mL hexane was added to the solution to precipitate the product, the solid product washed with hexane and dried *in vacuo*. Yield = 79%, 40 mg. The crystals suitable for X-ray diffraction were obtained by layering the benzene solution of the title compound with hexane at room temperature.

^{1}H NMR (400 MHz, C_6D_6). δ 8.34−8.22 (m, 4H, Ar−H), 7.88−7.76 (m, 4H, Ar−H), 7.44−7.33 (m, 2H, Ar−H), 7.11−6.97 (m, 8H, Ar−H), 6.95−6.85 (m, 6H, Ar−H), 6.76 (t, *J* = 7.6 Hz, 2H Ar−H), 1.25 (s, 3H, Xantphos CH_3), 1.15 (s, 3H, Xantphos CH_3), −15.06 - −15.47 (m, 1H, Rh−H), −18.60 to −18.99 (m, 1H, Rh−H).

$^{31}P\{^1H\}$ NMR (160 MHz, C_6D_6). δ 37.3 [d, $^1J_{RhP}$ = 117 Hz].

Microanalysis. $C_{39}H_{34}ClOP_2Rh$ (719.00) requires: C 65.15, H 4.77; found: C 65.33, H 4.66.

***mer*-[Rh(κ^3-$_{P,O,P}$-Xantphos)(η^2-PhCCPh)][BAr^F_4] 6.** To a flask containing **4** (175 mg), Na[BAr^F_4] (212 mg, 0.24 mmol, 1 equiv. relative to Rh), diphenyl acetylene (51 mg, 0.29 mmol, 1.2 equiv. relative to Rh) was added 15 mL 1,2-difluorobenzene, the resulting solution was stirred for 3 h at room temperature. The solution was filtered, and the filtrate was concentrated to dryness under vacuum, the resulting residue washed with pentane, then recrystallized by diffusion of pentane into a dichloromethane solution of the crude product at −18 °C to yield orange crystals. Yield = 82%, 340 mg.

^{1}H NMR (400 MHz, CD_2Cl_2). δ 7.82 (d, *J* = 7.6 Hz, 2H, Ar−H), 7.74−7.71 (m, 8H BAr^F_4), 7.55 (br, 4H BAr^F_4), 7.45 (d, *J* = 7.6 Hz, 4H Ar−H), 7.40 (t, *J* = 8.0 Hz, 2H Ar−H), 7.33−7.24 (m, 14H Ar−H), 7.15 (t, *J* = 7.2 Hz, 10H Ar−H), 7.02 (t, *J* = 7.6 Hz, 4H Ar−H), 1.86 (s, 6H, Xantphos CH_3).

$^{31}P\{^1H\}$ NMR (160 MHz, CD_2Cl_2). δ 20.4 [d, $^1J_{RhP}$ = 124 Hz].

ESI-MS (CH_2Cl_2) Positive Ion. $[M]^+$ *m*/*z* = 859.18 (calc. 859.18).

Microanalysis. $C_{85}H_{54}BF_{24}OP_2Rh$ (1722.99) requires: C 59.25, H 3.16; found: C 59.17, H 3.05.

***mer*-[Rh(κ^3-$_{P,O,P}$-Xantphos)(ClCH$_2$Cl)(σ,σ-(C_6H_4)C(H)═CPh)][BAr^F_4] (7).** **1a** (246 mg, 0.15 mmol) was dissolved in dichloromethane (5 mL), and the solution was exposed to H_2 for 30 min (1 atm). Then the solution was degassed by evaporation to dryness, diphenylacetylene (107 mg, 0.60 mmol) in CH_2Cl_2 (5 mL) added, and the mixture was stirred for 1h. The solution was evaporated and washed with hexane, The solid product was recrystallized with dichloromethane and hexane at −18 °C. Total yield =70%, 180 mg. The two products **6** and [Rh(κ^3-POP-Xantphos)(ClCH$_2$Cl)(σ,σ-(C_6H_4)C(H)═CPh)][BAr^F_4] **7** were observed by NMR spectrocopy, the ratio being 1:2 respectively. Crystals of **7** suitable for X-ray diffraction were obtained from dichloromethane solution with pentane at −18 °C.

^{1}H NMR (400 MHz, CD_2Cl_2). δ 8.00 (d, *J* = 7.6 Hz, 2H), 7.77−7.69 (m, 8H BAr^F_4), 7.60−7.13 (m, 25H), 7.00 (t, *J* = 7.6 Hz, 4H), 6.79−6.70 (m, 4H), 6.48 (t, *J* = 7.6 Hz, 1H), 6.38 (d, *J* = 2.8 Hz,, 1H), 6.21 (d, *J* = 7.2 Hz, 1H), 6.13 (t, *J* = 7.6 Hz, 1H), 6.05−6.01 (m, 1H), 2.11 (s, 3H, Xantphos CH_3), 1.70 (s, 3H, Xantphos CH_3). (coordinated dichloromethane was not observed.)

$^{31}P\{^1H\}$ NMR (160 MHz, CD_2Cl_2). δ 27.2 [d, $^1J_{RhP}$ = 119 Hz].

ESI-MS (CH_2Cl_2) Positive Ion. $[M]^+$ *m*/*z* = 859.17 (calc. 859.18).

[Rh(κ^3-$_{P,O,P}$-Xantphos)(σ,κ^1-C_6H_4COMe)(SMe)][BAr^F_4] (8). A solution of **6** (8 mg, 4.6 × 10^{-3}) and 2-(methylthio)acetophenone in D-toluene (0.5 mL) was prepared in a J. Young NMR tube and analyzed in situ by NMR spectroscopy at room temperature. A mixture of *mer*-[Rh(κ^3-POP-Xantphos)(σ,κ^1-C_6H_4COMe)(SMe)][BAr^F_4] (*mer*-**8**) and fac-[Rh(κ^3-POP-Xantphos)(σ,κ^1-C_6H_4COMe)(SMe)][BAr^F_4] (*fac*-**8**) was formed in the ratio of 1:20 after 20 min. The ratio of *fac*-**8** increased continually, so that after 32 h *fac*-**8** was the only observed Rh complex.

mer-**8** can be isolated in pure form with the following procedure:

To a J. Youngs tube containing **6** (258 mg, 0.15 mmol), 1-(2-(methylthio)phenyl)ethanone (55 mg, 0.33 mmol) was added 5 mL toluene, sealed and the resulting solution was stirred for 40 min at 100 °C. The solution was concentrated to dryness under vacuum, the resulting residue washed with pentane, then recrystallized by diffusion of pentane into a 1,2-difluorobenzene solution of the crude product at −18 °C to yield orange crystals. Yield = 70%, 180 mg.

Data for *mer*-8. *^{1}H NMR (400 MHz, CD_2Cl_2).* δ 8.06 (d, *J* = 8.0 Hz, 1H, Ar−H), 7.93 (dd, *J* = 7.6 Hz, *J* = 2.0 Hz 2H, Ar−H), 7.82−7.76 (m, 4H Ph), 7.74−7.70 (m, 8H BAr^F_4), 7.62−7.47 (m, 10H Ar−H + BAr^F_4), 7.47−7.39 (m, 5H Ar−H), 7.33 (t, *J* = 7.6 Hz, 2H Ph′), 7.26

DOI: 10.1021/om500984y
Organometallics 2015, 34, 711−723

(dd, J = 8.0 Hz, J = 1.6 Hz, 1H, Ar−H), 7.18−7.11 (m, 5H), 6.71−6.64 (m, 4H, Ph′) 1.99 (s, COMe 3H), 1.78 (s, Xantphos CH_3 3H), 1.32 (s, Xantphos CH_3 3H), 0.87 (s, SMe 3H).

$^{31}P\{^1H\}$ NMR (160 MHz, CD_2Cl_2). δ 23.8 [d, $^1J_{RhP}$ = 106 Hz].

ESI-MS (CH_2Cl_2) Positive Ion. $[M]^+$ m/z = 847.14 (calc. 847.14).

Microanalysis. $C_{80}H_{54}BF_{24}O_2P_2RhS$ (1710.99) requires: C 56.16, H 3.18; found: C 55.93, H 3.16.

Data for *fac*-8. *^1H NMR (400 MHz, D-Toluene).* δ 8.37−6.09 (m, 42H), 1.56 (d, J = 7.6 Hz, 3H, SMe), 1.48 (s, Xantphos CH_3, 3H), 1.43 (d, J = 1.2 Hz, 3H), 1.39 (s, Xantphos CH_3, 3H).

$^{31}P\{^1H\}$ NMR (160 MHz, D-Toluene). δ 34.8 [dd, $^1J_{RhP}$ = 150 Hz, $^2J_{PP}$ = 17 Hz], 22.6 [dd, $^1J_{RhP}$ = 104 Hz, $^2J_{PP}$ = 17 Hz].

***mer*-[Rh(κ^3-$_{P,O,P}$-Xantphos)(σ,κ^1-C_6H_4COOMe)(SMe)][BAr^F_4] (9).** To a J. Youngs tube containing **6** (100 mg, 0.06 mmol), methyl 2-(methylsulfanyl)benzoate (13 mg, 0.07 mmol) was added 10 mL chlorobenzene, sealed and the resulting solution was stirred for 30 min at 80 °C. The solution was concentrated to dryness under vacuum, the resulting residue washed with pentane, then recrystallized by diffusion of pentane into a dichloromethane solution of the crude product at −18 °C to yield brown crystals. Yield =77%, 80 mg.

^1H NMR (400 MHz, CD_2Cl_2). δ 8.00 (d, J = 8.0 Hz, 1H, Ar−H), 7.94 (d, J = 7.2 Hz, 2H, Ar−H), 7.90−7.81 (m, 4H Ph), 7.74−7.71 (m, 8H BAr^F_4), 7.64−7.51 (m, 10H Ar−H + BAr^F_4), 7.49−7.41 (m, 5H Ar−H), 7.36 (t, J = 6.8 Hz, 3H Ar−H), 7.26−7.11 (m, 5H Ar−H), 6.77−6.69 (m, 4H, Ph′) 2.82 (s, COOMe 3H), 1.96 (s, Xantphos Me 3H), 1.82 (s, Xantphos Me 3H), 0.85 (s, SMe 3H).

$^{31}P\{^1H\}$ NMR (160 MHz, CD_2Cl_2). δ 22.2 [d, $^1J_{RhP}$ = 106 Hz].

ESI-MS (CH_2Cl_2) Positive Ion. $[M]^+$ m/z = 863.14 (calc. 863.14).

Microanalysis. $C_{80}H_{54}BF_{24}O_3P_2RhS$ (1726.99) requires: C 55.64, H 3.15; found: C 55.55, H 3.07.

***mer*-[Rh(κ^3-$_{P,O,P}$-Xantphos)(σ,κ^1-$C_6H_4NO_2$)(SMe)][BAr^F_4] (10).** To a flask containing **6** (100 mg, 0.06 mmol), 2-nitrothioanisole (10 mg, 0.06 mmol) was added 15 mL dichloromethane, the resulting solution was stirred for 24 h room temperature. The solution was concentrated to dryness under vacuum, the resulting residue washed with pentane, then recrystallized by diffusion of pentane into a 1,2-difluorobenzene solution of the crude product at −18 °C to yield brown crystals. Yield = 66%, 68 mg.

^1H NMR (400 MHz, CD_2Cl_2). δ 8.14 (d, J = 8.0 Hz, 1H, Ar−H), 7.96−7.94 (m, 2H), 7.79−7.68 (m, 12H, Ar−H + BAr^F_4), 7.65−7.54 (m, 11H Ar−H + BAr^F_4), 7.47 (t, J = 7.6 Hz, 4H Ar−H), 7.39−7.34 (m, 3H Ar−H), 7.21 (t, J = 7.6 Hz, 1H Ar−H), 7.15 (t, J = 7.6 Hz, 4H Ar−H), 6.81−6.75 (m, 4H, Ph′), 1.98 (s, Xantphos Me 3H), 1.77 (s, Xantphos Me 3H), 0.88 (s, SMe 3H).

$^{31}P\{^1H\}$ NMR (160 MHz, CD_2Cl_2). δ 23.1 [d, $^1J_{RhP}$ = 102 Hz].

ESI-MS (CH_2Cl_2) Positive Ion. $[M]^+$ m/z = 850.12 (calc. 850.12).

Microanalysis. $C_{78}H_{51}BF_{24}NO_3P_2RhS$ (1713.95) requires: C 54.66, H 3.00, N 0.82; found: C 54.57, H 2.87, N 0.86.

***mer*−[Rh(κ^3-$_{P,O,P}$-Xantphos)(σ,κ^1-2-(2-oxazolinyl)phenyl)-(SMe)][BAr^F_4] (11).** To a J. Youngs tube containing **6** (100 mg, 0.06 mmol), 2-(2-(methylthio)phenyl-4,5-dihydrooxazole (14 mg, 0.07 mmol) was added 10 mL chlorobenzene, sealed and the resulting solution was stirred for 60 min at 100 °C. The solution was concentrated to dryness under vacuum, the resulting residue washed with pentane, then recrystallized by diffusion of pentane into a dichloromethane solution of the crude product at −18 °C to yield orange crystals. Yield =78%, 81 mg.

^1H NMR (400 MHz, CD_2Cl_2). δ 7.99−7.86 (m, 7H), 7.76−7.69 (m, 8H, BAr^F_4), 7.67−7.55 (m, 8H Ar−H + BAr^F_4), 7.51 (t, J = 7.6 Hz, 2H Ar−H), 7.44−7.30 (m, 8H Ar−H), 7.29−7.20 (m, 5H Ar−H), 6.72−6.63 (m, 4H, Ph), 3.32 (t, J = 9.6 Hz, 2H oxazoline CH_2), 2.35 (t, J = 9.6 Hz, 2H oxazoline CH_2), 1.94 (s, Xantphos Me 3H), 1.72 (s, Xantphos Me 3H), 0.84 (s, SMe 3H).

$^{31}P\{^1H\}$ NMR (160 MHz, CD_2Cl_2). δ 17.8 [d, $^1J_{RhP}$ = 103 Hz].

ESI-MS (CH_2Cl_2) positive ion. $[M]^+$ m/z = 874.16 (calc. 874.15).

Microanalysis. $C_{81}H_{55}BF_{24}NO_2P_2RhS$ (1738.02) requires: C 55.98, H 3.19, N 0.81; found: C 56.04, H 3.09, N 0.78.

***mer*-[Rh(κ^3-$_{P,O,P}$-Xantphos)(σ,κ^1-2-(2-pyridyl)phenyl)(SMe)]-[BAr^F_4] (12).** To a J. Youngs tube containing **6** (25 mg, 0.015 mmol), 2-(2-(methylthio)phenylpyridine (4 mg, 0.02 mmol) was added 10 mL chlorobenzene, sealed and the resulting solution was stirred for 3 h at 80 °C. The solution was concentrated to dryness under vacuum, the resulting residue washed with pentane, then recrystallized by diffusion of pentane into a dichloromethane and toluene mixture solution of the crude product at −18 °C to yield red crystals. Yield = 69%, 18 mg.

^1H NMR (400 MHz, CD_2Cl_2). δ 8.05 (d, J = 7.6 Hz, 1H), 7.96 (dd, J = 7.2 Hz, J = 1.6 Hz 2H), 7.91−7.82 (m, 4H), 7.76−7.70 (m, 8H BAr^F_4), 7.64−7.12 (m, 20H), 7.12−7.03 (m, 3H), 6.82 (t, J = 7.6 Hz, 4H), 6.43−6.34 (m, 4H, Ph), 1.92 (s, Xantphos Me 3H), 1.90 (s, Xantphos Me 3H), 0.88 (s, SMe 3H).

$^{31}P\{^1H\}$ NMR (160 MHz, CD_2Cl_2). δ 20.1 [d, $^1J_{RhP}$ = 105 Hz].

ESI-MS (CH_2Cl_2) Positive Ion. $[M]^+$ m/z = 882.16 (calc. 882.16).

Microanalysis. $C_{83}H_{55}BF_{24}NOP_2RhS$ (1746.04) requires: C 57.10, H 3.19, N 0.80; found: C 57.20, H 3.16, N 0.87.

***fac*-[Rh(κ^3-$_{P,O,P}$-Xantphos)(η^3-C_3H_5)(SPh)][BAr^F_4] (13).** To a J. Youngs tube containing **6** (100 mg, 0.06 mmol), allyl phenyl sulfide (19 mg, 0.12 mmol) was added 10 mL chlorobenzene, sealed and the resulting solution was stirred for 2 h at 80 °C. The solution was concentrated to dryness under vacuum, the resulting residue washed with pentane, then recrystallized by diffusion of pentane into a dichloromethane solution of the crude product at −18 °C to yield green crystals. Yield = 60%, 61 mg.

^1H NMR (400 MHz, CD_2Cl_2). δ 7.88−7.78 (m, 4H), 7.77−7.62 (m, 10H), 7.66−7.48 (m, 14H), 7.23−7.12 (m, 3H), 7.08−6.99 (m, 4H), 6.92−6.88 (m, 4H), 6.82 (t, J = 7.6 Hz, 2H), 6.66 (d, J = 7.6 Hz, 2H), 4.80 (quintet, J = 10.0 Hz, 1H CH C_3H_5), 4.05−3.93 (m, 2H CH_2 C_3H_5), 2.71−2.57 (m, 2H CH_2 C_3H_5), 1.95 (s, Xantphos Me 3H), 1.30 (s, Xantphos Me 3H).

$^{31}P\{^1H\}$ NMR (160 MHz, CD_2Cl_2). δ 22.7 [d, $^1J_{RhP}$ = 132 Hz].

ESI-MS (CH_2Cl_2) Positive Ion. $[M]^+$ m/z = 831.15 (calc. 831.15).

Microanalysis. $C_{80}H_{54}BF_{24}OP_2RhS$ (1695.00) requires: C 56.69, H 3.21; found: C 56.84, H 3.17.

***mer*-[Rh(κ^3-$_{P,O,P}$-Xantphos)(σ,κ^1-(COMe)C_6H_3SMe)(H)][BAr^F_4] (14).** To a J. Youngs tube containing **6** (80 mg, 0.046 mmol), 4-(methylthio)acetophenone (11.5 mg, 0.069 mmol) was added 10 mL toluene, the resulting solution was stirred for 2 days at room temperature. The solution was filtered, and then concentrated to dryness under vacuum, the resulting residue washed with pentane, then recrystallized by diffusion of pentane into a chlorobenzene solution of the crude product at −18 °C to yield colorless crystals. Yield =38%, 30 mg.

^1H NMR (400 MHz, CD_2Cl_2). δ 8.02−7.94 (m, 4H), 7.79 (dd, J = 7.6 Hz, J = 2.0 Hz 3H), 7.77−7.68 (m, 9H), 7.63−7.56 (m, 10H), 7.47−7.35 (m, 6H), 7.24−7.17 (m, 7H), 6.78 (dd, J = 8.4 Hz, J = 1.6 Hz, 1H), 6.69−64 (m, 3H), 2.33 (s, 3H), 1.86 (s, 3H), 1.77 (s, 3H), 1.43 (s, 3H), −14.99 (dt, J_{RhH} = 29.2 Hz, J_{PH} = 10.8 Hz, 1H)

$^{31}P\{^1H\}$ NMR (160 MHz, CD_2Cl_2). δ 39.5 [d, $^1J_{RhP}$ = 114 Hz].

ESI-MS (Acetone) Positive Ion. $[M]^+$ m/z = 847.15 (calc. 847.15).

Microanalysis. $C_{80}H_{54}BF_{24}O_2P_2RhS$ (1710.99) requires: C 56.16, H 3.18; found: C 56.38, H 3.01.

Crystallography. X-ray crystallography data were collected on an Agilent SuperNova diffractometer using graphite monochromated Cu Kα radiation (λ = 1.54180 Å), or an Enraf Nonius Kappa CCD diffractometer using Mo Kα radiation (λ = 0.71073 Å) with the use of low-temperature devices [150(2) K].[61] Data were reduced using the instrument manufacturer software, DENZO-SMN,[62,63] and CrystalClear. All structures were solved *ab initio* using SIR92,[64] or SuperFlip,[65] and the structures were refined using CRYSTALS[66] or SHELX.[67] All non-hydrogen atoms were refined with anisotropic displacement parameters. All hydrogen atoms were placed in calculated positions using the riding model unless otherwise stated. Crystallographic data have been deposited with the Cambridge Crystallographic Data Center under CCDC 1025603−1025612. These data can be obtained free of charge from The Cambridge Crystallographic Data Center via www.ccdc.cam.ac.uk/data_request/cif.

DOI: 10.1021/om500984y
Organometallics 2015, 34, 711−723

■ ASSOCIATED CONTENT

Supporting Information

Details of the crystallographic refinement, with CIF files giving positional and displacement parameters, crystallographic data, and bond lengths and angles. This material is available free of charge via the Internet at http://pubs.acs.org.

■ AUTHOR INFORMATION

Corresponding Author

*E-mail: andrew.weller@chem.ox.ac.uk.

Present Address

†(P.R.) Department of Chemistry, Princeton, NJ 08544, USA.

Notes

The authors declare no competing financial interest.

■ ACKNOWLEDGMENTS

The Swiss National Science Foundation (postdoctoral fellowship for P.R.); the EPSRC (DTG award to S.D.P., EP/K505031/1); the Archimedes Foundation (Estonia) for a Ph.D. Scholarship (I.P.); Amit Kumar for assistance with ESI−MS measurements; E. J. Emmett and R. J. Pawley for preliminary synthetic studies.

■ REFERENCES

(1) Van Der Boom, M. E.; Milstein, D. *Chem. Rev.* **2003**, *103*, 1759−1792.
(2) Morales-Morales, D.; Jensen, C. M. *The Chemistry of Pincer Compounds*; Elsevier: Amsterdam, 2007.
(3) Albrecht, M. *Chem. Rev.* **2010**, *110*, 576−623.
(4) Choi, J.; MacArthur, A. H. R.; Brookhart, M.; Goldman, A. S. *Chem. Rev.* **2011**, *111*, 1761−1779.
(5) van Koten, G.; Milstein, D. *Organometallic Pincer Chemistry*; Springer: Heidelberg, 2013.
(6) Kranenburg, M.; van der Burgt, Y. E. M.; Kamer, P. C. J.; Van Leeuwen, P. W. N. M.; Goubitz, K.; Fraanje, J. *Organometallics* **1995**, *14*, 3081−3089.
(7) Freixa, Z.; Van Leeuwen, P. W. N. M. *Dalton Trans.* **2003**, 1890−1901.
(8) Sandee, A. J.; van der Veen, L. A.; Reek, J.; Kamer, P.; Lutz, M.; Spek, A. L.; van Leeuwen, P. *Angew. Chem., Int. Ed.* **1999**, *38*, 3231−3235.
(9) Williams, G. L.; Parks, C. M.; Smith, C. R.; Adams, H.; Haynes, A.; Meijer, A. J.; Sunley, G. J.; Gaemers, S. *Organometallics* **2011**, *30*, 6166−6179.
(10) Dallanegra, R.; Chaplin, A. B.; Weller, A. S. *Organometallics* **2012**, *31*, 2720−2728.
(11) Haibach, M. C.; Wang, D. Y.; Emge, T. J.; Krogh-Jespersen, K.; Goldman, A. S. *Chem. Sci.* **2013**, *4*, 3683−3692.
(12) Esteruelas, M. A.; Olivan, M.; Vélez, A. *Inorg. Chem.* **2013**, *52*, 5339−5349.
(13) Esteruelas, M. A.; Olivan, M.; Vélez, A. *Inorg. Chem.* **2013**, *52*, 12108−12119.
(14) Julian, L. D.; Hartwig, J. F. *J. Am. Chem. Soc.* **2010**, *132*, 13813−13822.
(15) Pawley, R. J.; Moxham, G. L.; Dallanegra, R.; Chaplin, A. B.; Brayshaw, S. K.; Weller, A. S.; Willis, M. C. *Organometallics* **2010**, *29*, 1717−1728.
(16) Johnson, H. C.; Mcmullin, C. L.; Pike, S. D.; Macgregor, S. A.; Weller, A. S. *Angew. Chem., Int. Ed.* **2013**, *52*, 9776−9780.
(17) Johnson, H. C.; Leitao, E. M.; Whittell, G. R.; Manners, I.; Lloyd-Jones, G. C.; Weller, A. S. *J. Am. Chem. Soc.* **2014**, *136*, 9078−9093.
(18) Johnson, H. C.; Torry-Harris, R.; Ortega, L.; Theron, R.; McIndoe, J. S.; Weller, A. S. *Catal. Sci. Technol.* **2014**, *4*, 3486−3494.
(19) Arambasic, M.; Hooper, J. F.; Willis, M. C. *Org. Lett.* **2013**, *15*, 5162−5165.
(20) Hooper, J. F.; Chaplin, A. B.; González-Rodríguez, C.; Thompson, A. L.; Weller, A. S.; Willis, M. C. *J. Am. Chem. Soc.* **2012**, *134*, 2906−2909.
(21) Jones, W. D. *Inorg. Chem.* **2005**, *44*, 4475−4484.
(22) Wang, L.; He, W.; Yu, Z. *Chem. Soc. Rev.* **2012**, *42*, 599−621.
(23) Barbero, N.; Martin, R. *Org. Lett.* **2012**, *14*, 796−799.
(24) Pan, F.; Shi, Z.-J. *ACS Catal.* **2013**, *4*, 280−288.
(25) Hooper, J. F.; Young, R. D.; Pernik, I.; Weller, A. S.; Willis, M. C. *Chem. Sci.* **2013**, *4*, 1568−1572.
(26) Modha, S. G.; Mehta, V. P.; Van der Eycken, E. V. *Chem. Soc. Rev.* **2013**, *42*, 5042−5055.
(27) Liu, X.-Y.; Venkatesan, K.; Schmalle, H. W.; Berke, H. *Organometallics* **2004**, *23*, 3153−3163.
(28) Wilson, A. D.; Miller, A. J. M.; DuBois, D. L.; Labinger, J. A.; Bercaw, J. E. *Inorg. Chem.* **2010**, *49*, 3918−3926.
(29) Thomas, R.; Lakshmi, S.; Pati, S. K.; Kulkarni, G. U. *J. Phys. Chem. B* **2006**, *110*, 24674−24677.
(30) Ghosh, R.; Zhang, X.; Achord, P.; Emge, T. J.; Krogh-Jespersen, K.; Goldman, A. S. *J. Am. Chem. Soc.* **2007**, *129*, 853−866.
(31) Werner, H.; Wolf, J.; Schubert, U.; Ackermann, K. *J. Organomet. Chem.* **1986**, *317*, 327−356.
(32) Choudhury, J.; Pratihar, S.; Maity, A. K.; Roy, S. *Can. J. Chem.* **2009**, *87*, 183−187.
(33) Huhmann-Vincent, J.; Scott, B. L.; Kubas, G. J. *Inorg. Chem.* **1999**, *38*, 115−124.
(34) Taw, F. L.; Mellows, H.; White, P. S.; Hollander, F. J.; Bergman, R. G.; Brookhart, M.; Heinekey, D. M. *J. Am. Chem. Soc.* **2002**, *124*, 5100−5108.
(35) Krumper, J. R.; Gerisch, M.; Suh, J. M.; Bergman, R. G.; Tilley, T. D. *J. Org. Chem.* **2003**, *68*, 9705−9710.
(36) Kornecki, K. P.; Briones, J. F.; Boyarskikh, V.; Fullilove, F.; Autschbach, J.; Schrote, K. E.; Lancaster, K. M.; Davies, H. M. L.; Berry, J. F. *Science* **2013**, *342*, 351−354.
(37) Corkey, B. K.; Taw, F. L.; Bergman, R. G.; Brookhart, M. *Polyhedron* **2004**, *23*, 2943−2954.
(38) Amini, M.; Bagherzadeh, M.; Moradi-Shoeili, Z.; Boghaei, D. M. *RSC Adv.* **2012**, *2*, 12091−12095.
(39) Pawley, R. J.; Huertos, M. A.; Lloyd-Jones, G. C.; Weller, A. S.; Willis, M. C. *Organometallics* **2012**, *31*, 5650−5659.
(40) Perutz, R. N.; Sabo-Etienne, S. *Angew. Chem., Int. Ed.* **2007**, *46*, 2578−2592.
(41) Moxham, G. L.; Randell-Sly, H.; Brayshaw, S. K.; Weller, A. S.; Willis, M. C. *Chem.—Eur. J.* **2008**, *14*, 8383−8397.
(42) Leñero, K. Q. A.; Guari, Y.; Kamer, P. C. J.; van Leeuwen, P. W. N. M.; Donnadieu, B.; Sabo-Etienne, S.; Chaudret, B.; Lutz, M.; Spek, A. L. *Dalton Trans.* **2013**, *42*, 6495−6512.
(43) Bakhmutov, V. I.; Bozoglian, F.; Gómez, K.; González, G.; Grushin, V. V.; Macgregor, S. A.; Martin, E.; Miloserdov, F. M.; Novikov, M. A.; Panetier, J. A.; Romashov, L. V. *Organometallics* **2011**, *31*, 1315−1328.
(44) Hua, R.; Takeda, H.; Onozawa, S.-y.; Abe, Y.; Tanaka, M. *Org. Lett.* **2007**, *9*, 263−266.
(45) Miyauchi, Y.; Watanabe, S.; Kuniyasu, H.; Kurosawa, H. *Organometallics* **1995**, *14*, 5450−5453.
(46) Johns, A. M.; Utsunomiya, M.; Incarvito, C. D.; Hartwig, J. F. *J. Am. Chem. Soc.* **2006**, *128*, 1828−1839.
(47) Kakiuchi, F.; Murai, S. *Acc. Chem. Res.* **2002**, *35*, 826−834.
(48) Hartwig, J. F. *OrganoTransition Metal Chemistry*; University Science Books: 2010.
(49) Widegren, J. A.; Finke, R. G. *J. Mol. Catal. A* **2003**, *198*, 317−341.
(50) Yamada, M.; Shen, Z.; Miyake, M. *Chem. Commun.* **2006**, 2569−2571.
(51) Gacem, N.; Diao, P. *Colloid Surf. A* **2013**, *417*, 32−38.
(52) Pangborn, A. B.; Giardello, M. A.; Grubbs, R. H.; Rosen, R. K.; Timmers, F. J. *Organometallics* **1996**, *15*, 1518−1520.
(53) Buschmann, W. E.; Miller, J. S. *Inorg. Synth.* **2002**, *33*, 83−84.
(54) Ent, A. v. d.; Onderdelinden, A. L. *Inorg. Synth.* **1990**, *33*, 90−91.

DOI: 10.1021/om500984y
Organometallics 2015, 34, 711−723

(55) Abel, E. W.; Bennett, M. A.; Wilkinson, G. *J. Chem. Soc.* **1959**, 3178−3182.
(56) Emmett, E. J.; Hayter, B. R.; Willis, M. C. *Angew. Chem., Int. Ed.* **2013**, *52*, 12679−12683.
(57) Hooper, J. F.; Young, R. D.; Weller, A. S.; Willis, M. C. *Chem.—Eur. J.* **2013**, *19*, 3125−3130.
(58) Chen, X.; Hao, X.-S.; Goodhue, C. E.; Yu, J.-Q. *J. Am. Chem. Soc.* **2006**, *128*, 6790−6791.
(59) Lubben, A. T.; McIndoe, J. S.; Weller, A. S. *Organometallics* **2008**, *27*, 3303−3306.
(60) Majek, M.; von Wangelin, A. J. *Chem. Commun.* **2013**, *49*, 5507−5509.
(61) Cosier, J.; Glazer, A. M. *J. Appl. Crystallogr.* **1986**, *19*, 105−107.
(62) Otwinowski, Z.; Minor, W. *Macromol. Cryst. A* **1997**, *276*, 307−326.
(63) *Crysalis Pro*; Oxford Diffraction: 2011.
(64) Altomare, A.; Burla, M. C.; Camalli, G.; Cascarano, G.; Giacovazzo, C.; Gualiardi, A.; Polidori, G. *J. Appl. Crystallogr.* **1994**, *27*, 435−435.
(65) Palatinus, L.; Chapuis, G. *J. Appl. Crystallogr.* **2007**, *40*, 786−786.
(66) Betteridge, P. W.; Carruthers, J. R.; Cooper, R. I.; Prout, K.; Watkin, D. J. *J. Appl. Crystallogr.* **2003**, *36*, 1487−1487.
(67) Sheldrick, G. M. *Acta Crystallogr.* **2008**, *A64*, 112−112.

DOI: 10.1021/om500984y
Organometallics 2015, 34, 711−723